3

Electromagnetic Waves in Crystals with Metallized Boundaries

V.I. Alshits[1,2], V.N. Lyubimov[1], and A. Radowicz[3]
[1]*A.V. Shubnikov Institute of Crystallography, Russian Academy of Sciences, Moscow, 119333*
[2]*Polish-Japanese Institute of Information Technology, Warsaw, 02-008*
[3]*Kielce University of Technology, Kielce, 25-314*
[1]*Russia*
[2,3]*Poland*

1. Introduction

The metal coating deposited on the surface of a crystal is a screen that locks the electromagnetic fields in the crystal. Even for a real metal when its complex dielectric permittivity ε_m has large but finite absolute value, electromagnetic waves only slightly penetrate into such coating. For example, for copper in the wavelength range $\lambda = 10^{-5}$–10^{-3} cm, from the ultraviolet to the infrared, the penetration depth d changes within one order of magnitude: $d \approx 6 \times (10^{-8}$–$10^{-7})$ cm, remaining negligible compared to the wavelength, $d << \lambda$. In the case of a perfect metallization related to the formal limit $\varepsilon_m \to \infty$ the wave penetration into a coating completely vanishes, $d = 0$. The absence of accompanying fields in the adjacent space simplifies considerably the theory of electromagnetic waves in such media. It turned out that boundary metallization not only simplifies the description, but also changes significantly wave properties in the medium. For example, it leads to fundamental prohibition (Furs & Barkovsky, 1999) on the existence of surface electromagnetic waves in crystals with a positively defined permittivity tensor $\hat{\varepsilon}$. There is no such prohibition at the crystal–dielectric boundary (Marchevskii et al., 1984; D'yakonov, 1988; Alshits & Lyubimov, 2002a, 2002b)). On the other hand, localized polaritons may propagate along even perfectly metalized surface of the crystal when its dielectric tensor $\hat{\varepsilon}$ has strong frequency dispersion near certain resonant states so that one of its components is negative (Agranovich, 1975; Agranovich & Mills, 1982; Alshits et al., 2001; Alshits & Lyubimov, 2005). In particular, in the latter paper clear criteria were established for the existence of polaritons at the metalized boundary of a uniaxial crystal and compact exact expressions were derived for all their characteristics, including polarization, localization parameters, and dispersion relations.

In this chapter, we return to the theory of electromagnetic waves in uniaxial crystals with metallized surfaces. This time we will be concerned with the more common case of a crystal with a positively defined tensor $\hat{\varepsilon}$. Certainly, under a perfect metallization there is no localized eigenmodes in such a medium, but the reflection problem in its various aspects and such peculiar eigenmodes as the exceptional bulk (nonlocalized) polaritons that transfer energy parallel to the surface and satisfy the conditions at the metallized boundary remain.

We will begin with the theory for the reflection of plane waves from an arbitrarily oriented surface in the plane of incidence of the general position, where the reflection problem is solved by a three-partial superposition of waves: one incident and two reflected components belonging to different sheets of the refraction surface. However, one of the reflected waves may turn out to be localized near the surface. Two-partial reflections, including mode conversion and "pure" reflection, are also possible under certain conditions. The incident and reflected waves belong to different sheets of the refraction surface in the former case and to the same sheet of ordinary or extraordinary waves in the latter case. First, we will study the existence conditions and properties of pure (simple) reflections. Among the solutions for pure reflection, we will separate out a subclass in which the passage to the limit of the eigenmode of exceptional bulk polaritons is possible. Analysis of the corresponding dispersion equation will allow us to find all of the surface orientations and propagation directions that permit the existence of ordinary or extraordinary exceptional bulk waves. Subsequently, we will construct a theory of conversion reflections and find the configurations of the corresponding pointing surface for optically positive and negative crystals that specifies the refractive index of reflection for each orientation of the optical axis.
The mentioned theory is related to the idealized condition of perfect metallization and needs an extension to the case of the metal with a finite electric permittivity ε_m. The transition to a real metal may be considered as a small perturbation of boundary condition. As was initially suggested by Leontovich (see Landau & Lifshitz, 1993), it may be done in terms of the so called surface impedance $\zeta = 1/\sqrt{\varepsilon_m}$ of metal. New important wave features arise in the medium with $\zeta \neq 0$. In particular, a strongly localized wave in the metal (a so-called plasmon) must now accompany a stationary wave field in the crystal. In a real metal such plasmon should dissipate energy. Therefore the wave in a crystal even with purely real tensor $\hat{\varepsilon}$ must also manifest damping. In addition, in this more general situation the exceptional bulk waves transform to localized modes in some sectors of existence (the non-existence theorem (Furs & Barkovsky, 1999) does not valid anymore).
We shall consider a reaction of the initial idealized physical picture of the two independent wave solutions, the exceptional bulk wave and the pure reflection in the other branch, on a "switching on" the impedance ζ combined with a small change of the wave geometry. It is clear without calculations that generally they should loss their independency. The former exceptional wave cannot anymore exist as a one-partial eigenmode and should be added by a couple of partial waves from the other sheet of the refraction surface. But taking into account that the supposed perturbation is small, this admixture should be expected with small amplitudes. Thus we arise at the specific reflection when a weak incident wave excites, apart from the reflected wave of comparable amplitude from the same branch, also a strong reflected wave from the other polarization branch. The latter strong reflected wave should propagate at a small angle to the surface being close in its parameters to the initial exceptional wave in the unperturbed situation.
Below we shall concretize the above consideration to an optically uniaxial crystal with a surface coated by a normal metal of the impedance ζ supposed to be small. The conditions will be found when the wave reflection from the metallized surface of the crystal is of resonance character being accompanied by the excitation of a strong polariton-plasmon. The peak of excitation will be studied in details and the optimized conditions for its observation will be established. Under certain angles of incidence, a conversion occurs in the resonance

area: a pumping wave is completely transformed into a surface polariton--plasmon of much higher intensity than the incident wave. In this case, no reflected wave arises: the normal component of the incident energy flux is completely absorbed in the metal. The conversion solution represents an eigenmode opposite in its physical sense to customary leaky surface waves known in optics and acoustics. In contrast to a leaky eigenwave containing a weak «reflected» partial wave providing a leakage of energy from the surface, here we meet a pumped surface polariton-plasmon with the weak «incident» partial wave transporting energy to the interface for the compensation of energy dissipation in the metal.

2. Formulation of the problem and basic relations

Consider a semi-bounded, transparent optically uniaxial crystal with a metallized boundary and an arbitrarily oriented optical axis. Its dielectric tensor $\hat{\varepsilon}$ is conveniently expressed in the invariant form (Fedorov, 2004) as

$$\hat{\varepsilon} = \varepsilon_o \hat{I} + (\varepsilon_e - \varepsilon_o)\mathbf{c} \otimes \mathbf{c}\,, \tag{1}$$

where $\hat{I}$ is the identity matrix, $\mathbf{c}$ is a unit vector along the optical axis of the crystal, $\otimes$ is the symbol of dyadic product, ε_o and ε_e are positive components of the electric permittivity of the crystal. For convenience, we will use the system of units in which these components are dimensionless (in the SI system, they should be replaced by the ratios $\varepsilon_o/\varepsilon^0$ and $\varepsilon_e/\varepsilon^0$, where ε^0 is the permittivity of vacuum).

In uniaxial crystals, one distinguishes the branches of ordinary (with indices "o") and extraordinary (indices "e") electromagnetic waves. Below, along with the wave vectors $\mathbf{k}_\alpha$ ($\alpha = o, e$), we shall use dimensionless refraction vectors $\mathbf{n}_\alpha = \mathbf{k}_\alpha/k_0$ where $k_0 = \omega/c$, ω is the wave frequency and c is the light speed. These vectors satisfy the equations (Fedorov, 2004)

$$\mathbf{n}_o \cdot \mathbf{n}_o = \varepsilon_o\,, \qquad \mathbf{n}_e \cdot \hat{\varepsilon}\mathbf{n}_e = \varepsilon_o\varepsilon_e\,. \tag{2}$$

For real vectors $\mathbf{n}_o$ and $\mathbf{n}_e$, the ray velocities (the velocities of energy propagation) of the corresponding bulk waves are defined by

$$\mathbf{u}_o = \frac{c\mathbf{n}_o}{\varepsilon_o}, \qquad \mathbf{u}_e = \frac{c\hat{\varepsilon}\mathbf{n}_e}{\varepsilon_o\varepsilon_e} = \frac{c}{\varepsilon_o\varepsilon_e}\left[\varepsilon_o\mathbf{n}_e + (\varepsilon_e - \varepsilon_o)(\mathbf{n}_e \cdot \mathbf{c})\mathbf{c}\right]. \tag{3}$$

Formulas (3) show that, in the ordinary wave, energy is transported strictly along the refraction vector, whereas, in the extraordinary wave, generally not.

For our purposes, it is convenient to carry out the description in a coordinate system associated not with the crystal symmetry elements, but with the wave field parameters. Let us choose the x axis in the propagation direction $\mathbf{m}$ and the y axis along the inner normal $\mathbf{n}$ to the surface. In this case, the xy plane is the plane of incidence where all wave vectors of the incident and reflected waves lie, the xz plane coincides with the crystal boundary, and the optical axis is specified by an arbitrarily directed unit vector $\mathbf{c}$ (Fig. 1). The orientation of vector $\boldsymbol{c} = (c_1, c_2, c_3)$ in the chosen coordinate system can be specified by two angles, θ and φ. The angle θ defines the surface orientation and the angle φ on the surface defines the propagation direction of a stationary wave field.

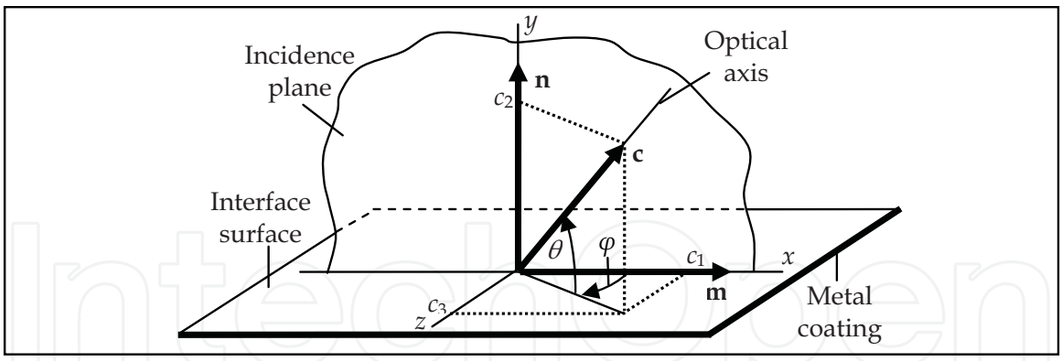

Fig. 1. The system of *xyz* coordinates and the orientation **c** of the crystal's optical axis

The stationary wave field under study can be expressed in the form:

$$\begin{pmatrix} \mathbf{E}(x,y,t) \\ \mathbf{H}(x,y,t) \end{pmatrix} = \begin{pmatrix} \mathbf{E}(y) \\ \mathbf{H}(y) \end{pmatrix} \exp[ik(x - vt)] . \tag{4}$$

The y dependence of this wave field is composed from a set of components. In the crystal ($y > 0$) there are four partial waves subdivided into incident (i) and reflected (r) ones from two branches, ordinary (o) and extraordinary (e):

$$\begin{pmatrix} \mathbf{E}(y) \\ \mathbf{H}(y) \end{pmatrix} = C_o^i \begin{pmatrix} \mathbf{E}_o^i(y) \\ \mathbf{H}_o^i(y) \end{pmatrix} + C_o^r \begin{pmatrix} \mathbf{E}_o^r(y) \\ \mathbf{H}_o^r(y) \end{pmatrix} + C_e^i \begin{pmatrix} \mathbf{E}_e^i(y) \\ \mathbf{H}_e^i(y) \end{pmatrix} + C_e^r \begin{pmatrix} \mathbf{E}_e^r(y) \\ \mathbf{H}_e^r(y) \end{pmatrix} . \tag{5}$$

Here the vector amplitudes are defined by

$$\begin{pmatrix} \mathbf{E}_o^{i,r}(y) \\ \mathbf{H}_o^{i,r}(y) \end{pmatrix} = \begin{pmatrix} \mathbf{e}_o^{i,r} \\ \mathbf{h}_o^{i,r} \end{pmatrix} \exp(\mp ip_o ky) , \tag{6}$$

$$\begin{pmatrix} \mathbf{E}_e^{i,r}(y) \\ \mathbf{H}_e^{i,r}(y) \end{pmatrix} = \begin{pmatrix} \mathbf{e}_e^{i,r} \\ \mathbf{h}_e^{i,r} \end{pmatrix} \exp[i(p \mp p_e)ky] . \tag{7}$$

In Eqs. (4)–(7), **E**, **e** and **H**, **h** are the electric and magnetic field strengths, k is the common x component of the wave vectors for the ordinary and extraordinary partial waves: $k = \mathbf{k}_o^{i,r} \cdot \mathbf{m} = \mathbf{k}_e^{i,r} \cdot \mathbf{m}$, $v = \omega/k$ is the tracing phase velocity of the wave, and $C_o^{i,r}$ and $C_e^{i,r}$ are the amplitude factors to be determined from the boundary conditions. The upper and lower signs in the terms correspond to the incident and reflected waves, respectively.

In the isotropic metal coating ($y < 0$) only two partial waves propagate differing from each other by their *TM* and *TE* polarizations:

$$\begin{pmatrix} \mathbf{E}(y) \\ \mathbf{H}(y) \end{pmatrix} = \left(C_m^{TM} \begin{pmatrix} \mathbf{e}_m^{TM} \\ \mathbf{h}_m^{TM} \end{pmatrix} + C_m^{TE} \begin{pmatrix} \mathbf{e}_m^{TE} \\ \mathbf{h}_m^{TE} \end{pmatrix} \right) \exp(-ikp_m y) . \tag{8}$$

By definition, the above polarization vectors are chosen so that the *TM* wave has the magnetic component orthogonal to the sagittal plane and the electric field is polarized in

this plane, and for the *TE* wave, vice versa, the magnetic field is polarized in-plane and the electric field – out-plane:

$$\mathbf{h}_m^{TM} \| (0,0,1)\,,\ \ \mathbf{e}_m^{TM} \| \mathbf{n}_m \times \mathbf{h}_m^{TM}\,,\ \ \mathbf{e}_m^{TE} \| (0,0,1)\,,\ \ \mathbf{h}_m^{TE} \| \mathbf{n}_m \times \mathbf{e}_m^{TE}\,. \tag{9}$$

The refraction vectors of the partial waves in the superpositions (5) and (8) are equal

$$\mathbf{n}_o^{i,r} = n(1,\ \mp p_o,\ 0)^T\,,\quad \mathbf{n}_e^{i,r} = n(1,\ p \mp p_e,\ 0)^T\,,\quad \mathbf{n}_m = n(1,\ -p_m,\ 0)^T\,. \tag{10}$$

Here, the superscript T stands for transposition and $n = k/k_0 = c/v$ is the dimensionless wave slowness also called the refractive index. The parameters p_o, p_e, p and p_m that determine the dependences of the partial amplitudes on depth y can be represented as

$$p_o = \sqrt{s-1}\,,\quad p_e = \sqrt{\frac{\gamma}{A}\left(s - \frac{B}{A}\right)}\,,\quad p = (1-\gamma)\frac{c_1 c_2}{A}\,,\quad p_m = \frac{R}{\zeta n}\,, \tag{11}$$

where we use the notation

$$s = \varepsilon_o / n^2\,,\ \ \gamma = \varepsilon_e / \varepsilon_o\,,\quad A = 1 + c_2^2(\gamma - 1)\,,\ B = 1 - c_3^2(1 - 1/\gamma)\,, R = \sqrt{1 - (\zeta n)^2}\,. \tag{12}$$

The orientation of the polarization vectors in (5), (6) is known from (Born & Wolf, 1986; Landau & Lifshitz, 1993) and can be specified by the relations

$$\mathbf{e}_o^{i,r} \| \mathbf{n}_o^{i,r} \times \mathbf{c},\qquad \mathbf{e}_e^{i,r} \| \mathbf{n}_e^{i,r}(\mathbf{n}_e^{i,r} \cdot \mathbf{c}) - \boldsymbol{\varepsilon}_o \mathbf{c},\qquad \mathbf{h}_a^{i,r} = \mathbf{n}_a^{i,r} \times \mathbf{e}_a^{i,r}\,,\quad a = o, e\,. \tag{13}$$

Substituting relations (10) into (9) and (13) one obtains

$$\begin{pmatrix} \mathbf{e}_o^{i,r} \\ \mathbf{h}_o^{i,r} \end{pmatrix} = N_o^{i,r} \begin{pmatrix} (\mp p_o c_3,\ -c_3,\ c_2 \pm p_o c_1)^T \\ -n[p_o(p_o c_1 \pm c_2),\ \ c_2 \pm p_o c_1,\ \ c_3 s]^T \end{pmatrix}, \tag{14}$$

$$\begin{pmatrix} \mathbf{e}_e^{i,r} \\ \mathbf{h}_e^{i,r} \end{pmatrix} = N_e^{i,r} \begin{pmatrix} \{c_1 - [c_1 + (p \mp p_e)c_2]/s,\ \ c_2 - [c_1 + (p \mp p_e)c_2](p \mp p_e)/s,\ \ \ c_3\}^T \\ n[(p \mp p_e)c_3,\ \ \ -c_3,\ \ \ c_2 - (p \mp p_e)c_1]^T \end{pmatrix}, \tag{15}$$

$$\begin{pmatrix} \mathbf{e}_m^{TM} \\ \mathbf{h}_m^{TM} \end{pmatrix} = \begin{pmatrix} \zeta(R,\ \zeta n,\ 0)^T \\ (0,\ \ 0,\ \ 1)^T \end{pmatrix}, \qquad \begin{pmatrix} \mathbf{e}_m^{TE} \\ \mathbf{h}_m^{TE} \end{pmatrix} = \begin{pmatrix} (0,\ \ 0,\ -\zeta)^T \\ (R,\ \ \zeta n,\ \ 0)^T \end{pmatrix}. \tag{16}$$

The normalization in (14)-(16) was done from the conditions $|\mathbf{h}_{o,e}^{i,r}| = 1$ and $|\mathbf{h}_m^a| = 1$. It already presents in (16) and the factors $N_{o,e}$ in (14), (15) are specified by the equations

$$1/N_o^{i,r} = \sqrt{\varepsilon_o[(c_2 \pm c_1 p_o)^2 + c_3^2 s]}\,,\qquad 1/N_e^{i,r} = n\sqrt{1 + (p \mp p_e)^2 - [c_1 + c_2(p \mp p_e)]^2}\,. \tag{17}$$

3. Boundary conditions and a reflection problem in general statement

The stationary wave field (4) at the interface should satisfy the standard continuity conditions for the tangential components of the fields (Landau & Lifshitz, 1993):

$$\mathbf{E}_t\,|_{y=+0} = \mathbf{E}_t\,|_{y=-0}, \qquad \mathbf{H}_t\,|_{y=+0} = \mathbf{H}_t\,|_{y=-0}\,. \tag{18}$$

When the crystal is coated with perfectly conducting metal, the electric field in the metal vanishes and the boundary conditions (18) reduces to

$$\mathbf{E}_t\,|_{y=+0} = 0\,. \tag{19}$$

When the perfectly conducting coating is replaced by normal metal with sufficiently small impedance $\zeta = \zeta' + i\zeta''$ ($\zeta' > 0$, $\zeta'' < 0$), it is convenient to apply more general (although also approximate) Leontovich boundary condition (Landau & Lifshitz, 1993) instead of (19):

$$(\mathbf{E}_t + \zeta \mathbf{H}_t \times \mathbf{n})_{y=+0} = 0\,. \tag{20}$$

Below in our considerations, the both approximations, (19) and (20), will be applied. However we shall start from the exact boundary condition (18).

3.1 Generalization of the Leontovich approximation

The conditions (18) after substitution there equations (5)-(8) and (16) take the explicit form

$$\begin{pmatrix} e^r_{ox} & e^r_{ex} & \zeta R & 0 \\ e^r_{oz} & e^r_{ez} & 0 & -\zeta \\ h^r_{ox} & h^r_{ex} & 0 & R \\ h^r_{oz} & h^r_{ez} & 1 & 0 \end{pmatrix} \begin{pmatrix} C^r_o \\ C^r_e \\ C^{TM}_m \\ C^{TE}_m \end{pmatrix} = -C^i_o \begin{pmatrix} e^i_{ox} \\ e^i_{oz} \\ h^i_{ox} \\ h^i_{oz} \end{pmatrix} - C^i_e \begin{pmatrix} e^i_{ex} \\ e^i_{ez} \\ h^i_{ex} \\ h^i_{ez} \end{pmatrix}. \tag{21}$$

Following to (Alshits & Lyubimov, 2009a) let us transform this system for obtaining an exact alternative to the Leontovich approximation (20). We eliminate the amplitudes C^{TM}_m and C^{TE}_m of the plasmon in metal from system (21) and reduce it to the system of two equations:

$$\left[\begin{pmatrix} e^r_{ox} & e^r_{ex} \\ e^r_{oz} & e^r_{ez} \end{pmatrix} + \zeta \begin{pmatrix} -Rh^r_{oz} & -Rh^r_{ez} \\ h^r_{ox}/R & h^r_{ex}/R \end{pmatrix} \right] \begin{pmatrix} C^r_o \\ C^r_e \end{pmatrix} + \left[\begin{pmatrix} e^i_{ox} & e^i_{ex} \\ e^i_{oz} & e^i_{ez} \end{pmatrix} + \zeta \begin{pmatrix} -Rh^i_{oz} & -Rh^i_{ez} \\ h^i_{ox}/R & h^i_{ex}/R \end{pmatrix} \right] \begin{pmatrix} C^i_o \\ C^i_e \end{pmatrix} = 0\,. \tag{22}$$

Taking into account the matrix identities

$$\begin{pmatrix} -Rh^{i,r}_{oz} & -Rh^{i,r}_{ez} \\ h^{i,r}_{ox}/R & h^{i,r}_{ex}/R \end{pmatrix} = \begin{pmatrix} -h^{i,r}_{oz} & -h^{i,r}_{ez} \\ h^{i,r}_{ox} & h^{i,r}_{ex} \end{pmatrix} + (1-R) \begin{pmatrix} h^{i,r}_{oz} & h^{i,r}_{ez} \\ h^{i,r}_{ox}/R & h^{i,r}_{ex}/R \end{pmatrix} \tag{23}$$

and the explicit form of two-dimensional vectors $\mathbf{E}_t = (E_{tx}, E_{tz})^T$ and $\mathbf{H}_t = (H_{tx}, H_{tz})^T$ residing in the xz plane, namely

$$\mathbf{E}_t = C^i_o \begin{pmatrix} e^i_{ox} \\ e^i_{oz} \end{pmatrix} + C^r_o \begin{pmatrix} e^r_{ox} \\ e^r_{oz} \end{pmatrix} + C^i_e \begin{pmatrix} e^i_{ex} \\ e^i_{ez} \end{pmatrix} + C^r_e \begin{pmatrix} e^r_{ex} \\ e^r_{ez} \end{pmatrix}, \tag{24}$$

$$\mathbf{H}_t = C^i_o \begin{pmatrix} h^i_{ox} \\ h^i_{oz} \end{pmatrix} + C^r_o \begin{pmatrix} h^r_{ox} \\ h^r_{oz} \end{pmatrix} + C^i_e \begin{pmatrix} h^i_{ex} \\ h^i_{ez} \end{pmatrix} + C^r_e \begin{pmatrix} h^r_{ex} \\ h^r_{ez} \end{pmatrix}, \tag{25}$$

system (22) reduces to the following equation

$$\{\mathbf{E}_t + \zeta \mathbf{H}_t \times \mathbf{n} + \zeta(1-R)\hat{N}\mathbf{H}_t\}_{y=+0} = 0\,, \tag{26}$$

where the function $R(\zeta n)$ was defined in (12), and $\hat{N}(\zeta n)$ is the 2×2 matrix:

$$\hat{N}(\zeta n) = \begin{pmatrix} 0 & 1 \\ 1/R(\zeta n) & 0 \end{pmatrix}. \tag{27}$$

Notice that equation (26) is equivalent to an initial set of conditions (18). Impedance ζ in Eq. (26) is not assumed to be small and this expression only includes crystal fields (5)-(7). Thus, equation (26) is the natural generalization of Leontovich boundary condition (18).
However, the impedance ζ of ordinary metals (like copper or aluminum) may be considered as a small parameter, especially in the infrared range of wavelengths. In this case, function $R(\zeta n)$ in equation (26) [see in (12)] can be expanded in powers of the small parameter $(\zeta n)^2$, holding an arbitrary number of terms and calculating the characteristics of the wave fields with any desired precision. This expansion comprises odd powers of the parameter ζ:

$$\mathbf{E}_t + \zeta \mathbf{H}_t \times \mathbf{n} + \frac{1}{2}\zeta^3 n^2 \left(\hat{N}_1 + \sum_{s=1}^{\infty} (\zeta)^{2s} \frac{(2s-1)!!}{2^s (s+1)!} \hat{N}_{2s+1} \right) \mathbf{H}_t = 0\,, \tag{28}$$

where the set of matrices $\hat{N}_m$ ($m = 2s + 1$) is defined by the expression

$$\hat{N}_m = \begin{pmatrix} 0 & 1 \\ m & 0 \end{pmatrix}. \tag{29}$$

In view of our considerations, from expansion (28) it follows that the discrepancy between Leontovich approximation (20) and the exact boundary condition starts from the cubic term $\sim\zeta^3$; hence the quadratic corrections $\sim\zeta^2$ to the wave fields are correct in this approach.

3.2 Exact solution of the reflection problem

Now let us return to the reflection problem, i.e. to the system (21), which, together with relations (14) and (15), determines the amplitudes of superpositions (5) and (8). The right-hand side of (21) is considered to be known. When the reflection problem is formulated, only one incident wave is commonly considered by assuming its amplitude to be known (while the other is set equal to zero). The refractive index n, which directly determines the angle of incidence, is also assumed to be known, while the amplitudes of the reflected waves in the crystal and those of the plasmon components in the metal are to be determined.
Being here interested only in wave fields in the crystal, we can start our analysis from the more simple system (22) of only two equations with two unknown quantities. Omitting bulky but straightforward calculations we just present their results in the form of the reflection coefficients for the cases of an ordinary incident wave,

$$r_{oo} = \frac{C_o^r}{C_o^i} = -\frac{D(-p_o, p_e)N_o^i}{D(p_o, p_e)N_o^r}, \qquad r_{eo} = \frac{C_e^r}{C_o^i} = -\frac{D_{eo}N_o^i}{D(p_o, p_e)N_e^r}\,, \tag{30}$$

and an extraordinary incident wave,

$$r_{ee} = \frac{C_e^r}{C_e^i} = -\frac{D(p_o, -p_e)N_e^i}{D(p_o, p_e)N_e^r}, \qquad r_{oe} = \frac{C_o^r}{C_e^i} = -\frac{D_{oe}N_e^i}{D(p_o, p_e)N_o^r}. \tag{31}$$

In the above equations the following notation is introduced

$$\begin{aligned} D(p_o, p_e) = (c_1 p_o - c_2)(1 + p_o \zeta n / R)\{c_1 p_o^2 - c_2(p + p_e) - \zeta n R s[c_2 - c_1(p + p_e)]\} \\ + c_3^2 s(p_o + \zeta n R s)[1 + (p + p_e)\zeta n / R], \end{aligned} \tag{32}$$

$$D_{eo} = 2c_3 p_o s(1 - \varepsilon_o \zeta^2)(c_2 + c_1 \zeta n / R), \tag{33}$$

$$D_{oe} = 2c_3 p_e (1 - \varepsilon_o \zeta^2)(c_2 - c_1 \zeta n / R). \tag{34}$$

One can check that these expressions fit the known general equations (Fedorov & Filippov, 1976). Before beginning our analysis of Eqs. (30)-(34), recall that we consider only the crystals (and frequencies) that correspond to a positively defined permittivity tensor ($\varepsilon_o > 0$ and $\varepsilon_e > 0$). Depending on the relation between the components ε_o and ε_e, it is customary to distinguish the optically positive ($\varepsilon_e > \varepsilon_o$, i.e., $\gamma > 1$) and optically negative ($\varepsilon_e < \varepsilon_o$, i.e., $\gamma < 1$) crystals. Figure 2 shows the sections of the sheets of the refraction surface for these two types of crystals by the xy plane of incidence for arbitrary orientation of the boundary and propagation direction. Among the main reflection parameters shown in Fig. 2, the limiting values of the refractive indices $\hat{n}_o$ and $\hat{n}_e$ play a particularly important role:

$$\hat{n}_o = \sqrt{\varepsilon_o}, \qquad \hat{n}_e = \sqrt{\varepsilon_o A / B}. \tag{35}$$

These separate the regions of real and imaginary values of the parameters p_o and p_e:

$$p_o = \sqrt{(\hat{n}_o / n)^2 - 1}, \qquad p_e = \sqrt{[(\hat{n}_e / n)^2 - 1]\gamma B / A^2}. \tag{36}$$

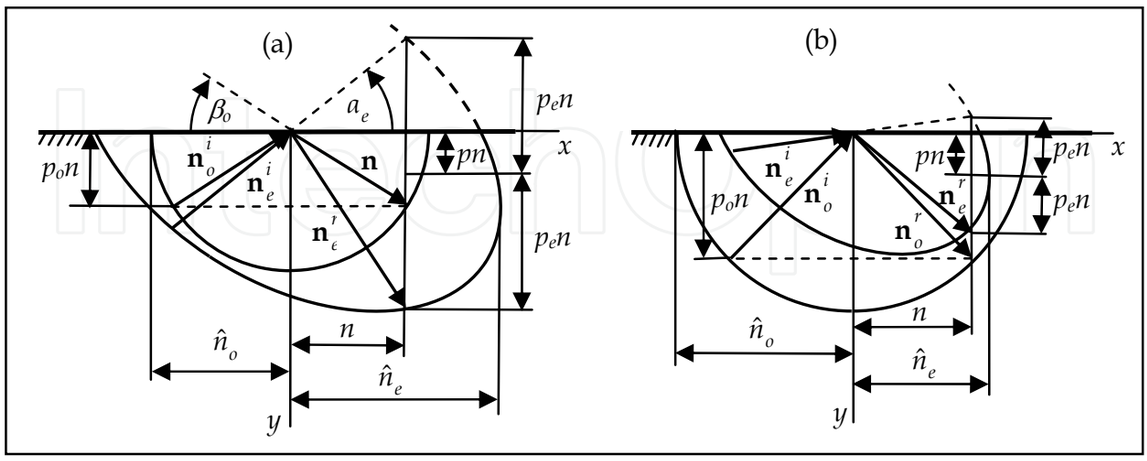

Fig. 2. Sections of the ordinary and extraordinary sheets of the refraction surface by the xy plane of incidence and main parameters of the reflection problem for optically positive (a) and optically negative (b) crystals

The parameter p_o remains real only in the region $0 \le n \le \hat{n}_o$, i.e., as long as the vertical straight line in Fig. 2 crosses the corresponding circular section of the spherical refraction sheet for ordinary waves (or touches it). Similarly, the parameter p_e remains real only in the region $0 \le n \le \hat{n}_e$. In both regions of real values, the refractive index $n = 0$ describes the reflection at normal incidence.

Thus, when the stationary wave motions along the surface are described, three regions of the refractive index n should be distinguished:

$$\text{(I) } 0 < n \le \min\{\hat{n}_o, \hat{n}_e\}, \text{ (II) } \min\{\hat{n}_o, \hat{n}_e\} < n \le \max\{\hat{n}_o, \hat{n}_e\}, \text{ (III) } n > \max\{\hat{n}_o, \hat{n}_e\}. \quad (37)$$

In the first region, both p_o and p_e are real — this is the region of reflections where all partial waves are bulk ones. This situation automatically arises in an optically positive crystal with an ordinary incident wave (Fig. 2a) or in an optically negative crystal with an extraordinary incident wave (Fig. 2b).

In region II, one of the parameters, p_o or p_e, is imaginary. This is p_o in an optically positive crystal and p_e in an optically negative one. Therefore, in the general solutions found below, one of the partial "reflected" waves may turn out to be localized near the surface. In particular, in this region, the amplitudes C_e^r (30) and C_o^r (31), respectively, in optically negative and positive crystals describe precisely these localized reflection components.

Finally, in region III, both parameters, p_o and p_e, are imaginary. In other words, in this region, a stationary wave field is possible in principle only in the form of surface electromagnetic eigenmodes — polaritons at fixed refractive index n specified by the poles of solutions (30) and (31), i.e., by the equation

$$D(n) = 0. \quad (38)$$

In this paper devoted mainly to the theory of reflection, only regions I and II (37) can be of interest to us. In principle, Eqs. (30) and (31) completely solve the reflection problem. In contrast to the problem of searching for eigenmodes, where the dispersion equation (38) specifying the admissible refractive indices n should be analyzed, the choice of n in the case of reflection only fixes the angle of incidence of the wave on the surface. In this case, the crystal cannot but react to the incident wave, while Eqs. (30) and (31) describe this reaction. However, the reflection has peculiar and sometimes qualitatively nontrivial features for certain angles of incidence. For example, the three-partial solution can degenerate into a two-partial one, so only one reflected wave belonging either to the same sheet of the refraction surface (simple reflection) or to the other sheet (mode conversion) remains instead of the two reflected waves. At the same time, when grazing incidence is approached, the total wave field either tends to zero or remains finite, forming a bulk polariton. Below, we will consider the mentioned features in more detail for the particular case of perfect metallization ($\zeta = 0$) when explicit analysis give visible results.

4. Specific features of wave reflection from the perfectly metallized boundary

The found above general expressions for reflection coefficients (30), (31) remain valid if to put into (32)-(34) $\zeta = 0$ and $R = 1$. As a result, we come to the much more compact functions

$$D(p_o, p_e) = (c_1 p_o - c_2)(c_1 g - c_2 p_e) + c_3^2 p_o \varepsilon_o / n^2, \quad (39)$$

$$D_{eo} = 2c_2c_3p_o\varepsilon_o / n^2, \tag{40}$$

$$D_{oe} = 2c_2c_3p_e, \tag{41}$$

where the new function $g(n)$ is introduced

$$g(n) = \frac{\varepsilon_o}{n^2} - \frac{1}{A} = p_o^2 - \frac{c_2}{c_1}p = \frac{A}{\gamma}\left(p_e^2 - \frac{c_3^2}{A^2}(\gamma - 1)\right). \tag{42}$$

With these simplifications we can proceed with our analysis basing on (Alshits et al., 2007).

4.1 Simple reflection

Let us consider the first type of two-partial reflections known as a pure (or simple) reflection. In this case the incident and reflected waves belong to the same refraction sheet, i.e., both components are either ordinary or extraordinary. It is obvious that such reflections take place when the amplitudes C_e^r in (30) or C_o^r in (31) become zero. This occurs when D_{oe} (40) or D_{eo} (41) vanishes, respectively. It is easily seen that both types of pure reflections are defined by the same criterion:

$$c_2\, c_3 = 0. \tag{43}$$

As follows from Eq. (43), the pure reflections of both ordinary and extraordinary waves in the crystals under consideration should exist independently of one another in the same two reflection geometries. This takes place only in those cases where the optical axis belongs either to the crystal surface ($c_2 = 0$) or to the plane of incidence ($c_3 = 0$). Since the optical axis in this case has a free orientation in these planes and since the angle of incidence is not limited by anything either, the pure reflections in three-dimensional space $\{n, \mathbf{c}\}$ occupy the surfaces defined as the set of two planes: $c_2 = 0$ and $c_3 = 0$. Let us consider in more detail the characteristics of pure reflections in these two geometries.

4.1.1 The optical axis parallel to the surface

In this case, $c_2 = 0$, i.e., $\theta = 0$, and the xy plane of incidence perpendicular to the surface makes an arbitrary angle φ with the direction of the optical axis. The main parameters for the independent reflections of ordinary and extraordinary waves take the form

$$\mathbf{n}_{o,e}^{i,r} = n\{1,\ \mp p_{o,e}(n),\ 0\}^T; \tag{44}$$

$$\begin{pmatrix} \mathbf{e}_o^{i,r} \\ \mathbf{h}_o^{i,r} \end{pmatrix} = \begin{pmatrix} (\pm c_3 p_o,\ c_3,\ \mp c_1 p_o)^T \\ n(c_1 p_o^2,\ \pm c_1 p_o,\ c_3\varepsilon_o / n^2)^T \end{pmatrix}, \quad \begin{pmatrix} \mathbf{e}_e^{i,r} \\ \mathbf{h}_e^{i,r} \end{pmatrix} = \begin{pmatrix} (c_1 p_o^2,\ \pm c_1 p_e,\ c_3\varepsilon_o / n^2)^T n / \varepsilon_o \\ (\mp c_3 p_e,\ -c_3,\ \pm c_1 p_e)^T \end{pmatrix}; \tag{45}$$

$$C_o^r = C_o^i, \qquad C_e^r = -C_e^i. \tag{46}$$

As above, the upper and lower signs in Eqs. (44) and (45) correspond to the incident (i) and reflected (r) waves, respectively. In Eq. (11) for $p_e(n)$, we should take into account the fact that $A = 1$ and $B = c_1^2 + c_3^2 / \gamma$ in this case. The angles of incidence are defined by $n < \hat{n}_{o,e}$. For brevity, the normalizing factors in Eqs. (45) are included in the amplitudes $C_{o,e}^{i,r}$.

Given (44)–(46), the pure reflection of the electric component of an ordinary wave in this geometry can be described by the combination

$$\mathbf{E}_o(x,y,t) = C_o\left(\mathbf{e}_o^i \exp(-ip_o ky) + \mathbf{e}_o^r \exp(ip_o ky)\right)\exp[ik(x-vt)]\,. \tag{47}$$

And the pure reflection of the magnetic component of an extraordinary wave is specified by a similar superposition:

$$\mathbf{H}_e(x,y,t) = C_e\left(\mathbf{e}_e^i \exp(-ip_e ky) - \mathbf{e}_e^r \exp(ip_e ky)\right)\exp[ik(x-vt)]. \tag{48}$$

4.1.2 The optical axis parallel to the plane of incidence

In this case, $c_3 = 0$, i.e., the azimuth $\varphi = 0$, while the angle θ is arbitrary, which corresponds to arbitrarily oriented crystal surface and plane of incidence passing through the optical axis. The main parameters of the independently reflected waves are given by the formulas

$$\mathbf{n}_o^{i,r} = n\{1,\ \mp p_o(n),\ 0\}^T\,, \qquad \mathbf{n}_e^{i,r} = n\{1,\ p \mp p_e(n),\ 0\}^T\,; \tag{49}$$

$$\begin{pmatrix} e_o^{i,r} \\ h_o^{i,r} \end{pmatrix} = \begin{pmatrix} (0,\ 0,\ 1)^T \\ n(\mp p_o,\ -1,\ 0)^T \end{pmatrix}, \qquad \begin{pmatrix} \mathbf{e}_e^{i,r} \\ \mathbf{h}_e^{i,r} \end{pmatrix} = \begin{pmatrix} (\pm p_e,\ \gamma / A^2 \pm p p_e,\ 0)^T \\ (0,\ 0,\ 1)^T \varepsilon_e / An \end{pmatrix}; \tag{50}$$

$$C_o^r = -C_o^i\,, \qquad C_e^r = C_e^i\,. \tag{51}$$

At $c_3 = 0$ in Eq. (11) for $p_e(n)$, we have $B = 1$ and $A = c_1^2 + \gamma c_2^2$. Thus, according to Eqs. (50), the pure reflection of ordinary waves is described by the partial *TE* modes with the electric component orthogonal to the sagittal plane. Similarly, the partial components of the pure reflection of extraordinary waves are formed by the *TM* modes with the magnetic component perpendicular to the same plane. In the case under consideration, the analogues of Eqs. (47) and (48) are even simpler:

$$\mathbf{E}_o(x,y,t) = C_o(0,\ 0,\ 1)\sin(p_o ky)\exp[ik(x-vt)]\,, \tag{52}$$

$$\mathbf{H}_e(x,y,t) = C_e(0,\ 0,\ 1)\cos(p_e ky)\exp[ik(x+py-vt)]\,. \tag{53}$$

4.2 Exceptional bulk polaritons

4.2.1 Simple reflections of ordinary waves at grazing incidence

As we see from Fig. 2, the grazing incidence of an ordinary wave is realized at $n = \hat{n}_o$, when, according to Eq. (36), $p_o = 0$. In this case, the simple reflection of an ordinary wave in the $c_2 = 0$ and $c_3 = 0$ planes behaves differently as grazing incidence is approached, $p_o \to 0$. As follows from Eqs. (44)–(46), in the former case where the optical axis is parallel to the surface ($c_2 = 0$), the incident and reflected partial waves at $p_o = 0$ are in phase and together form an ordinary exceptional bulk wave:

$$\begin{pmatrix} \mathbf{E}(x,t) \\ \mathbf{H}(x,t) \end{pmatrix} = C_o \begin{pmatrix} \mathbf{e}_o \\ \mathbf{h}_o \end{pmatrix} \exp\left(i\frac{\omega}{c}(\hat{n}_o x - ct) \right). \tag{54}$$

The refraction vector of the wave under consideration and its vector amplitude are

$$\mathbf{n}_o = (1,\ 0,\ 0)\hat{n}_o, \quad \hat{n}_o = \sqrt{\varepsilon_o}\,, \qquad \begin{pmatrix} \mathbf{e}_o \\ \mathbf{h}_o \end{pmatrix} = \begin{pmatrix} (0,\ 1,\ 0) \\ (0,\ 0,\ 1)\hat{n}_o \end{pmatrix}, \tag{55}$$

and the energy flux (Poynting vector) in this wave, $\mathbf{P}_o = \mathbf{E}_o \times \mathbf{H}_o$, lies at the intersection of the crystal surface with the sagittal surface, i.e., $\mathbf{P}_o \,||\, x$ (Fig. 3a).

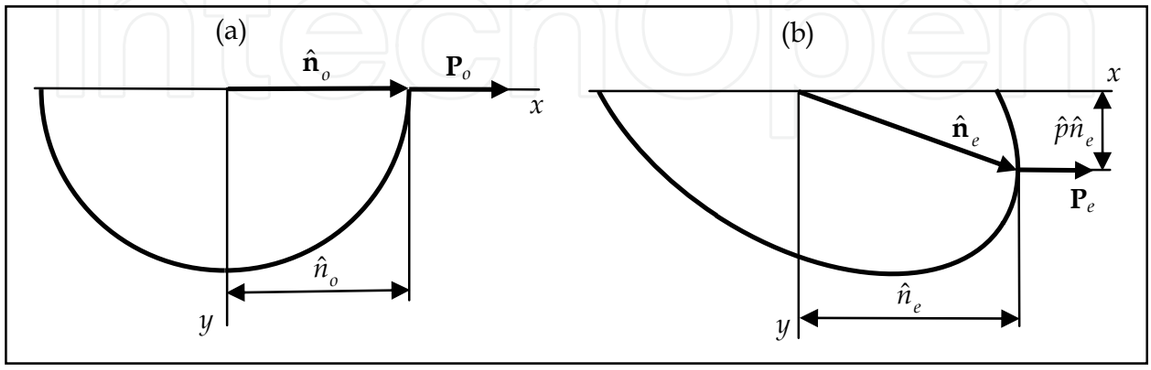

Fig. 3. Characteristics of the ordinary (a) and extraordinary (b) bulk polaritons that emerge at $c_2 = 0$ and $c_3 = 0$, respectively

On the other hand, the pure reflection of ordinary waves in the sagittal plane parallel to the optical axis ($c_3 = 0$, $c_2 \neq 0$) as grazing incidence is approached ($p_o \to 0$), according to Eqs. (52), gives antiphase incident and reflected partial waves that are mutually annihilated. In other words, no exceptional bulk polariton emerges on the branch of ordinary waves in this plane. The qualitative difference in the behavior of grazing incidence in the $c_2 = 0$ and $c_3 = 0$ planes that we found has a simple physical interpretation. For the limiting wave arising at grazing incidence to exist, its polarization $\mathbf{E}_o$, according to the boundary condition (19), must be orthogonal to the crystal surface, $\mathbf{E}_o \,||\, \mathbf{n} \,||\, y$. As we see from Eqs. (45), this is actually the case for an ordinary wave at $c_2 = 0$ and as $p_o \to 0$. However, the incident and reflected components in the sagittal plane, according to Eqs. (50) and (52), give polarization $\mathbf{E}_o$ that is not orthogonal, but parallel to the surface; hence the annihilation of these components.

4.2.2 Simple reflections of extraordinary waves at grazing incidence

The grazing incidence of extraordinary waves is considered similarly. It relates to $n \to \hat{n}_e$ and by (36), to $p_e \to 0$. In this case, the reverse is true: the incident and reflected waves are in antiphase (46) and, hence, are annihilated in the $c_2 = 0$ plane, and being in phase (51) when the optical axis is parallel to the sagittal ($c_3 = 0$) plane, which generates a bulk polariton:

$$\begin{pmatrix} \mathbf{E}(x,y,t) \\ \mathbf{H}(x,y,t) \end{pmatrix} = C_e \begin{pmatrix} \mathbf{e}_e \\ \mathbf{h}_e \end{pmatrix} \exp\left(i\frac{\omega}{c}[\hat{n}_e^0(x + py) - ct] \right), \tag{56}$$

where $\hat{n}_e^0$ is $\hat{n}_e$ taken at $c_3 = 0$ and $p_e = 0$. For the wave under consideration, we have

$$\mathbf{n}_e = (1,\ p,\ 0)\hat{n}_e^0, \quad \begin{pmatrix} \mathbf{e}_e \\ \mathbf{h}_e \end{pmatrix} = \begin{pmatrix} (0,\ 1,\ 0) \\ (0,\ 0,\ 1)\hat{n}_e^0 \end{pmatrix}, \tag{57}$$

$$\hat{n}_e^0 = \sqrt{\varepsilon_o A} = \sqrt{\varepsilon_o c_1^2 + \varepsilon_e c_2^2}\,,\ \ p = (\varepsilon_o - \varepsilon_e) c_1 c_2 \,/\, (\hat{n}_e^0)^2\,. \tag{58}$$

As we see from Eq. (57), the bulk polariton (56) is actually polarized in accordance with requirement (19): $\mathbf{e}_e \,||\, \mathbf{n}$. Note that the refraction vector $\mathbf{n}_e$ (57) is generally not parallel to the surface. But the Poynting vector of the wave $\mathbf{P}_e$ still lies at the intersection of the sagittal plane and the crystal surface, $\mathbf{P}_e \,||\, x$ (Fig. 3b). One can show that this is a general property of exceptional waves for $\zeta = 0$ holding even in biaxial crystals (Alshits & Lyubimov, 2009b).
In the special case of $c_2 = c_3 = 0$, which corresponds to the propagation direction x along the optical axis, the sheets of the ordinary and extraordinary waves of the refraction surface are in contact. As a result, degeneracy arises:

$$p_o = p_e = p = 0\,,\qquad \hat{n}_o = \hat{n}_e = \sqrt{\varepsilon_o}\,,\qquad \mathbf{n}_o = \mathbf{n}_e = (1,\ 0,\ 0)\,, \tag{59}$$

and solutions (54) and (56) merge, degenerating into the corresponding *TM* wave. Since the uniaxial crystal in the case under consideration is transversally isotropic, the orientation of the xy coordinate plane is chosen arbitrarily: for any fixed boundary parallel to the optical axis, a bulk wave with a polarization vector $\mathbf{E}_c$ orthogonal to the surface and an energy flux $\mathbf{P}_c \,||\, x$ can always propagate along the latter.

4.2.3 Proving the absence of other solutions

Thus, exceptional *ordinary* bulk polaritons (54) emerge when the optical axis is parallel to the crystal surface. At the same time, similar *extraordinary* eigenmodes (56) exist if the optical axis is parallel to the sagittal plane. In both cases, *TM*-type one-partial solutions with an energy flux $\mathbf{P}_{o,\,e}$ parallel to both the crystal surface and the sagittal plane occur (Fig. 3).
Let us show that the dispersion equation (38), (39),

$$D = (c_1 p_o - c_2)(c_1 g - c_2 p_e) + c_3^2 p_o (p_o^2 + 1) = 0 \tag{60}$$

has no other eigensolutions. In principle, an exceptional bulk polariton does not need to belong to the family of simple reflections. It could also be a two-partial one, i.e., consist of the bulk component of one branch corresponding to outer refraction sheet and the admixing localized component of the other branch. Examples of such mixed solutions are known both for crystals with a metallized surface [in the special case of $\varepsilon_o = 0$ and $\varepsilon_e > 0$ (Alshits & Lyubimov, 2005)] and at the open boundary of a crystal with a positively defined tensor $\hat{\varepsilon}$ (Alshits & Lyubimov, 2002a and 2002b). However, it is clear that any such wave with or without an admixture of inhomogeneous components carries energy parallel to the surface, i.e., its bulk component should have a zero parameter p_o or p_e (Fig. 3).
Substituting into (60) Eqs. (11) and (42) for p_e and g taken at $p_o = 0$,

$$c_2 (c_1 g - c_2 p_e) = 0\,, \tag{61}$$

it is easy to see that at $\gamma < 1$ the parameter g is real, while the parameter p_e is imaginary and, apart from the already known solution $c_2 = 0$, Eq. (60) has no other solutions, since the localization parameter p_e (11) does not become zero at $c_2 \neq 0$. At $\gamma > 1$, when p_e is also real, Eq. (60) is equivalent to the requirement

$$c_2^2 (c_2^2 + c_3^2) = 0\,, \tag{62}$$

which again leads to the solution $c_2 = 0$.
At $p_e = 0$, Eq. (60) takes the form

$$c_3^2[Ap_o + (\gamma - 1)c_1c_2] = 0\,, \tag{63}$$

where it is considered that $p_e = 0$ at $n = \hat{n}_e$ and, according to Eqs. (35) and (36),

$$p_o = \sqrt{(1-\gamma)(c_2^2 + c_3^2/\gamma)/A}\,. \tag{64}$$

This time the complexity in the dispersion equation (63) arises at $\gamma > 1$; the purely imaginary parameter p_o at $c_3 \neq 0$ does not become zero, so $c_3 = 0$ is the only root of Eq. (63). At $\gamma < 1$, it is convenient to rewrite Eq. (63) as

$$c_3^2\{\gamma^2c_2^2 + [1-(1-\gamma)^2c_2^2]\} = 0\,. \tag{65}$$

Since the expression in braces is positive at any direction of the optical axis, $c_3 = 0$ again remains the only root of the dispersion equation.
Thus, there are no new solutions for exceptional bulk polaritons other than the one-partial eigenmodes (54) and (56) in crystals with a perfectly metallized boundary found above.

4.3 Mode conversion at reflection

Let us now turn to the other, less common type of two-partial reflections where the wave incident on the surface is converted into the reflected wave of the "conjugate" polarization branch (i.e., belonging to the other refraction sheet). We pose the following question: Under what conditions does the mode conversion take place at reflection and what place do the orientation configurations allowing a two-partial reflection with the change of the refraction sheet occupy in the three-dimensional space $\{n, \theta, \varphi\}$ of all reflections? To answer this question, let us turn to solutions (30), (31), (39). Conversion arises for the incident ordinary wave if we choose the angle of incidence (or n) in such a way that $C_o^r = 0$ in (30), which is equivalent to the requirement $D(-p_o, p_e) = 0$. At the same time, according to (31), the incident extraordinary wave will turn into an ordinary wave at reflection if $D(p_o, -p_e) = 0$.

4.3.1 The equation for the conversion surface and its analytical solution

Here, one remark should be made. Clearly, the two-partial conversion reflection is reversible if the reflections from left to right and from right to left are kept in mind. We mean that the simultaneous reversal of the signs of the refraction vectors for the incident and reflected waves automatically converts the reflected wave into the incident one and the incident wave into the reflected one. Certainly, this reversed reflection is mathematically equivalent to the original one — the so-called reciprocity principle (Landau & Lifshitz, 1993). Symbolically, this can be written in the form: $o \rightarrow e = o \leftarrow e$. It is much less obvious that two conversion reflections in one direction, $o \rightarrow e$ and $e \rightarrow o$ (see Fig. 2), also satisfy the boundary conditions for the same geometry of the problem (i.e., the set $\{n, \mathbf{c}\}$).
Thus, the form of the conversion wave superpositions is determined by the equations

$$D_o \equiv -D(-p_o, p_e) \equiv (c_1 p_o + c_2)(c_1 g - c_2 p_e) + c_3^2 p_o (p_o^2 + 1) = 0\,, \tag{66}$$

$$D_e \equiv D(p_o, -p_e) \equiv (c_1 p_o - c_2)(c_1 g + c_2 p_e) + c_3^2 p_o (p_o^2 + 1) = 0\,, \tag{67}$$

which are not identical and one would think that they should specify two different sheets, $n = n_{o\to e}(\mathbf{c})$ and $n = n_{e\to o}(\mathbf{c})$, of the mode conversion surface. However, this is not the case. As we will show below, these sheets merge into one common conversion surface $n = n(\mathbf{c})$.
It is convenient to represent the sought-for mode conversion surface as the locus of points located at distance n from the coordinate origin along each $\mathbf{c}$ corresponding to the roots of Eqs. (66) and (67). From physical considerations, this surface should not go beyond region I (37). Let us prove that the physical roots n of Eqs. (66) and (67) belonging to region I are common ones. After certain transformations, they can be reduced to

$$D_{o,e} = \frac{g - p_o p_e}{1-\gamma}\left\{ f(z) \mp c_1 c_2 (\gamma - 1) \right\} = 0\,, \tag{68}$$

where the upper sign corresponds to the first subscript, the function $f(z)$ is defined by

$$f(z) = \frac{[A(1-c_2^2)p_o^2 + \gamma c_2^2 + c_3^2](g + p_o p_e)}{[c_1^2 g + c_3^2 (p_o^2 + 1)]p_o + c_2^2 p_e}\,, \tag{69}$$

and p_o, p_e, and g are the known functions (11) and (42) of the variable $z = n / \sqrt{\varepsilon_o} \equiv 1/\sqrt{s}$. It can be shown that the positive function $f(z)$ decreases monotonically in the domains of its existence $0 < z < 1$ (at $\gamma > 1$) or $0 < z < A/B < 1$ (at $\gamma < 1$). Since it is larger in absolute value than the second term on the right-hand side of Eq. (68) in the upper limit, i.e., $f(z_{\max}) > |c_1 c_2 (\gamma - 1)|$, the expression in braces in (68) has no physical roots. Thus, the two complex irrational equations (66) and (67) can be reduced to one simple equation:

$$g - p_o p_e = 0\,. \tag{70}$$

This implies that the mode conversion surface is actually a single-sheet one and the processes $o \to e$ and $e \to o$ are represented in space by the same pointing surface.
In the given domain of the variable z, one has $g + p_o p_e > 0$ and the following identity holds:

$$\frac{g - p_o p_e}{1-\gamma} = \frac{g^2 - p_o^2 p_e^2}{(1-\gamma)(g + p_o p_e)} = \frac{A^2[(c_1^2 + c_2^2)z^4 - (c_1^2 + A)z^2 + A(c_1^2 + c_3^2)]}{g + p_o p_e}\,. \tag{71}$$

Therefore, Eq. (70) is equivalent to the biquadratic equation

$$(c_1^2 + c_2^2)z^4 - (c_1^2 + A)z^2 + A(c_1^2 + c_3^2) = 0\,. \tag{72}$$

Thus, we arrive at a compact exact analytical form of the conversion surface $n = n(\mathbf{c})$:

$$n = n_{\pm}(\mathbf{c}) = \sqrt{\frac{\varepsilon_o}{2(1-c_3^2)}\left(c_1^2 + A \pm \sqrt{(c_1^2 - A)^2 - 4A c_2^2 c_3^2} \right)}\,, \tag{73}$$

on which, however, additional condition I (37) was superimposed. As we see from this solution, the surface under study is very symmetric. It is invariant with respect to the

change of sign of any component of vector **c**, i.e., it has three mutually orthogonal symmetry planes coincident with the coordinate planes. However, the main property of this surface is that each point of it describes two different conversion reflections, $o \to e$ and $e \to o$. In other words, the following assertion is valid:

If a two-partial wave reflection with the change of the refraction sheet (e.g., $o \to e$) exists in the geometry under consideration, then the other conversion reflection ($e \to o$) should also be at the same orientations of the boundary (θ) and the reflection plane (φ) and the same refractive index (n).

Analysis shows that the shape of the mode conversion surface is significantly different for optically positive ($\gamma > 1$) and negative ($\gamma < 1$) crystals. This is clearly seen from Fig. 4, where surface (73) was constructed numerically at $\gamma = 1.5$ (a) and 0.8 (b). Because of symmetry, we show only the upper halves ($c_2 > 0$) of the corresponding surfaces from which the quarters ($0 < \varphi < \pi/2$) were cut out for clarity. For an optically positive crystal, the conversion surface has the shape of an axially asymmetric torus in which the hole shrinks to the point coincident with the coordinate origin. This surface is a single-sheet one in the sense that the ray along each vector **c** crosses it once.

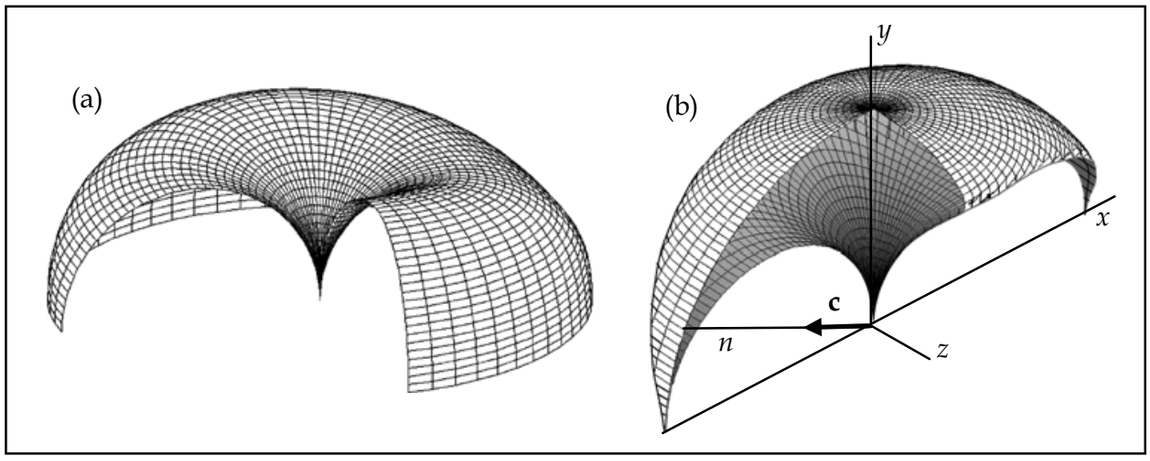

Fig. 4. Conversion surfaces for an optically positive crystal with $\gamma = 1.5$ (a) and an optically negative crystal with $\gamma = 0.8$ (b)

The conversion surface for a negative crystal is radically different: it is a two-sheet one (the ray along **c** crosses it twice); the upper half of the surface resembles a mushroom with a cap that descends to the x axis on both sides and a stipe that sharpens downward.

To analyze in more detail the geometry of the conversion surfaces of the above two types, it is convenient to consider their sections by the $c_1 = 0$, $c_2 = 0$, and $c_3 = 0$ coordinate planes.

4.3.2 The section of the conversion surface by the $c_1 = 0$ coordinate plane

In this section, the azimuth φ is fixed ($\varphi = \pi/2$ and $3\pi/2$) and solution (73) takes the form

$$n = n_{\pm}(\theta) = \sqrt{\frac{\varepsilon_o}{2\sin^2\theta}\left(A \pm \sqrt{A(A - \sin^2 2\theta)}\right)}, \qquad A = 1 + (\gamma - 1)\sin^2\theta\,. \tag{74}$$

According to condition I (37), the closed $n = n_{\pm}(\theta)$ curves should not go beyond the circle:

$$n \le \min\{\sqrt{\varepsilon_o}, \sqrt{\varepsilon_e}\}\,. \tag{75}$$

It is easy to verify that n_+ lies outside region (75) for optically positive crystals ($\gamma > 1$) at any angle θ, i.e., $n_+(\theta) > \sqrt{\varepsilon_o}$, while n_- belongs to this region at all θ: $n_-(\theta) < \sqrt{\varepsilon_o}$. Thus, the root n_+ should be discarded at $\gamma > 1$; this explains why the surface $n(\mathbf{c})$ is a single-sheet one at $\gamma > 1$. Thus, the sought-for section of the conversion surface by the $c_1 = 0$ plane is

$$n = n_-(\theta) = \sqrt{\frac{\varepsilon_o A}{2\sin^2\theta}\left(1 - \sqrt{1 - \frac{\sin^2 2\theta}{A}}\right)}. \tag{76}$$

Curiously enough, as $\gamma = \varepsilon_e/\varepsilon_o$ (the crystal anisotropy) increases, solution (76) tends to a limiting function that does not depend on γ,

$$n \approx n_-^{\gamma >> 1}(\theta) = \sqrt{\varepsilon_o}\,|\cos\theta|\,, \tag{77}$$

and that is represented by two circumferences with radius $\sqrt{\varepsilon_o}/2$ touching one another at the coordinate origin with a common tangent along the y axis (see Fig. 5a). However, most crystals have a small rather than large anisotropy, when $\gamma - 1 << 1$, and solution (76) is close to another limiting function:

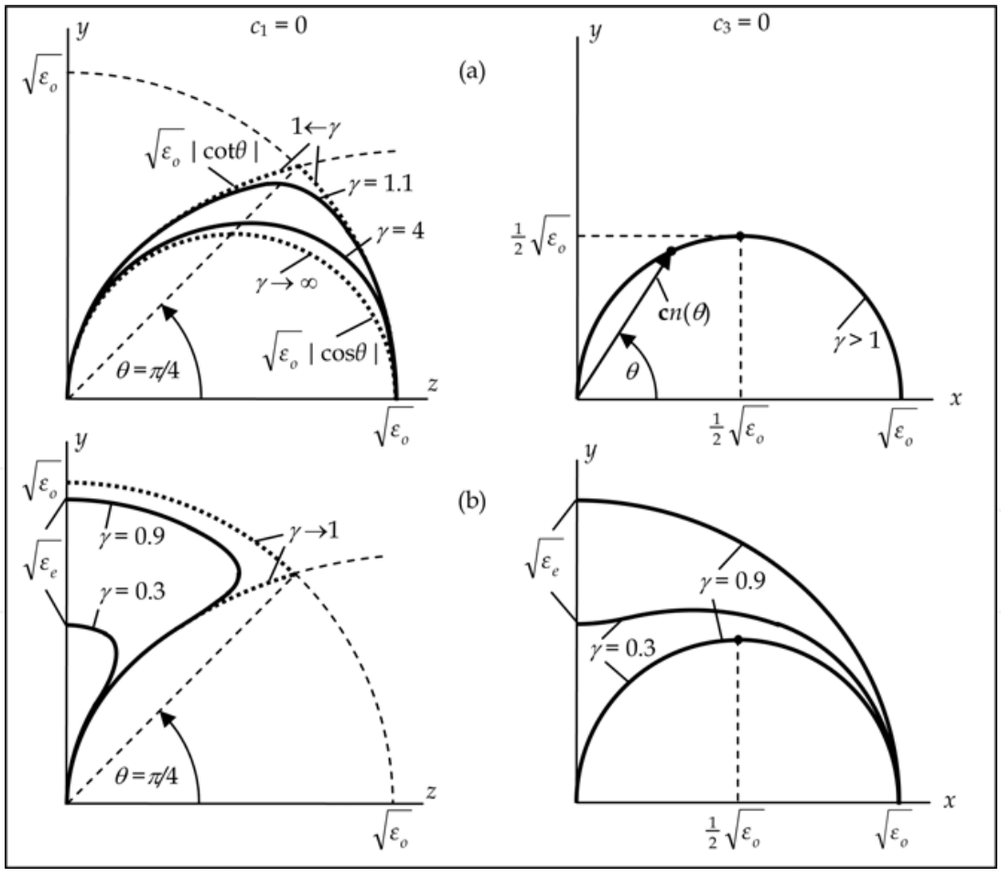

Fig. 5. Sections of the conversion surfaces $n(\mathbf{c})$ by the $c_1 = 0$ and $c_3 = 0$ planes for optically positive (a) and optically negative (b) crystals (given the symmetry of the surfaces $n(\mathbf{c})$ relative to the coordinate planes, the region is bounded by the interval $0 \le \theta \le \pi/4$)

$$n \approx n_{-}^{\gamma \approx 1}(\theta) = \begin{cases} \sqrt{\varepsilon_o}, & |\theta| \le \pi/4; \\ \sqrt{\varepsilon_o}\,|\cot\theta|, & |\theta| \ge \pi/4, \end{cases} \tag{78}$$

which coincides with the large circumference $\hat{n}_o(\theta) = \sqrt{\varepsilon_o}$ in the region $|\theta| \le \pi/4$ and approaches to the small circumferences (77) near the coordinate origin (see Fig. 5a). As we see from the same figure, the $n(\theta)$ curves corresponding to $\gamma = 4$ and 1.1 actually approach the limiting curves (77) and (78).

For an optically negative crystal ($\gamma < 1$), by no means any orientation of vector **c** satisfies the requirement that (74) be real and condition (75), which is now reduced to the inequality $n_{\pm}(\theta) \le \hat{n}_e = \sqrt{\varepsilon_e}$. On the other hand, both branches of solution (74), $n_{-}(\theta)$ and $n_{+}(\theta)$, are valid in this case in the region of allowed angles θ, so the surface becomes a two-sheet one. Naturally, the configuration of the section of the conversion surface differs significantly from that in the case of $\gamma > 1$ considered above (see the $c_1 = 0$ sections in Fig. 5b).

Let us now consider Eq. (74) in the special case of a small anisotropy, $0 < 1 - \gamma << 1$, which is practically realized in most crystals. Formally, this solution is very similar to (78)

$$n = n_{\pm}(\theta) \approx \begin{cases} \sqrt{\varepsilon_o}, & |\theta| \ge \pi/4, \\ \sqrt{\varepsilon_o}\,|\cot\theta|, & |\theta| \ge \pi/4. \end{cases} \tag{79}$$

This time, however, the limiting solution exists only in the region $|\theta| \ge \pi/4$, where the inner branch $n_{-}(\theta)$ closely follows Eq. (78). At $|\theta| = \pi/4$, the transition to the large circumference again occurs (Fig. 5b), but upward, to the outer branch $n_{+}(\theta)$, rather than downward. Here, it should be noted that we do not distinguish εo from εe in (78) with our accuracy of the zero-order approximation in parameter $1 - \gamma$. However, we can show that including the next expansion terms ensures that the inequality $n_{\pm} \le \hat{n}_e$ is satisfied.

Note also yet another circumstance important for the subsequent analysis. A check indicates that the curvature of the $c_1 = 0$ section under consideration remains positive for a negative crystal at the upper and lower points ($\theta = \pm\pi/2$) in the entire region $0 < \gamma < 1$.

4.3.3 The sections of the conversion surface by the planes of simple reflection

Curiously enough, the conversion surface under study also intersects with the other two coordinate planes, $c_3 = 0$ and $c_2 = 0$, which, as we know, are the planes of simple reflection. The physical interpretation of the paradoxical existence of such "antagonistic" reflection modes will be given below.

The $c_3 = 0$ section ($\varphi = 0$ and $\varphi = \pi$). In the $c_3 = 0$ coordinate plane, Eqs. (66) and (67) are simplified via factorization, although they appear different. However, given the identity

$$c_1 g \pm c_2 p_e = \frac{p_e(c_1^2 p_o^2 - c_2^2)}{c_1 p_e \mp c_2 \gamma / A}, \tag{80}$$

which is valid at $c_3 = 0$, both Eqs. (66) and (67) in this plane can be reduced to

$$p_e(c_1^2 p_o^2 - c_2^2) = 0. \tag{81}$$

The first root of this equation that corresponds to the requirement $p_e = 0$ and that is equal to

$$n = \hat{n}_e(\theta) = \sqrt{\varepsilon_o \cos^2\theta + \varepsilon_e \sin^2\theta}\ , \tag{82}$$

belongs to region I (37) (being its boundary) only at $\gamma < 1$. We are talking about the one-partial eigensolutions (54), which can turn into the two-partial superposition corresponding either to a pure reflection at grazing incidence or to a conversion reflection at certain small perturbations of the geometry of the problem. In the latter case, an ordinary bulk (incident or reflected) wave with small amplitude is admixed to a weakly perturbed original extraordinary component.

For optically positive crystals ($\gamma > 1$), solution (82) lies outside region I (37) bounded by the circumference with radius $n = \hat{n}_o$ and is extraneous, because p_o is a purely imaginary parameter at $n > \hat{n}_o$ and the exceptional bulk polariton under consideration cannot turn into a conversion reflection at any small perturbation (i.e., (82) is not part of the conversion surface). The fact that the other two factors in Eq. (82) become zero, $c_1 p_o - c_2 = 0$ and $c_1 p_o + c_2 = 0$, leads to the combined solution

$$n = \hat{n}_o |\cos\theta|\,, \qquad \varphi = 0,\ \pi\,. \tag{83}$$

It coincides with the asymptotic solution (77) in the $c_1 = 0$ section and has a simple graphical representation in polar coordinates (n, θ) in the form of two circumferences with radius $\hat{n}_o/2$ symmetric relative to the x and y coordinate axes and touching one another at the coordinate origin (see the $c_3 = 0$ section in Fig. 5a). Thus, at large γ the conversion surface has identical circular sections in the $c_1 = 0$ and $c_3 = 0$ sections. A check shows that at $\gamma >> 1$ any other sections of the conversion surface by the planes passing through the y axis are described by the same Eq. (83). In other words, the corresponding limiting surface $n(\mathbf{c})$ should have the shape of an ideal circular torus.

It is easy to verify that the pair of circumferences (83) entirely belongs to region I (37) at any γ. For optically positive crystals ($\gamma > 1$), this trivially follows from the comparison of Eq. (83) with the equality $\hat{n}_o = \sqrt{\varepsilon_o}$ (see (35)). However, it is also satisfied at any θ for optically negative crystals ($\gamma < 1$), for which condition I (37) is reduced to the more binding inequality $n < \hat{n}_e(\theta)$. This becomes obvious if we write this condition as

$$\sqrt{\varepsilon_o}\,|\cos\theta| < \sqrt{\varepsilon_o \cos^2\theta + \varepsilon_e \sin^2\theta}\ . \tag{84}$$

Certainly, at $\gamma < 1$ solution (83) should be complemented by root (72) obtained above, which is in agreement with the conversion surface being a two-sheet one. As we see from Fig. 5b ($c_3 = 0$), the outer part of the section described by function (82) changes the sign of the curvature at the upper and lower points ($\theta = \pm\pi/2$) as the parameter γ passes through a certain critical value γ_0. A simple calculation gives $\gamma = 1/2$ for the zero-curvature parameter. As we saw, the curvature remains universally positive at any γ for optically negative crystals in the $c_1 = 0$ section in the vicinity of the same direction. This means that the conversion surface in the direction $\mathbf{c} \,||\, y$ remains convex only at $1/2 < y < 1$ and has a saddle point at $0 < \gamma < 1/2$.

The physical meanings of solutions (82) and (83) differ significantly. In contrast to the boundary one-partial solution corresponding to (82), Eq. (83) specifies a two-partial reflection, which however, has its own peculiarities. The condition $c_3 = 0$ implies that the

optical axis belongs to the plane of incidence and that the reflections described by Eq. (83) correspond to the two specific situations where the direction of either the incident wave or the reflected one coincides with the optical axis (see Fig. 6). The equations $c_1 p_o - c_2 = 0$ and $c_1 p_o + c_2 = 0$ are satisfied in the former and latter cases, respectively. In a sense, the two-partial reflections of this kind with one of the components belonging to both refraction sheets are simultaneously simple and conversion ones. Therefore, the intersection of the conversion surface with the $c_3 = 0$ plane along lines (83) contains no paradox.

As we see from Fig. 6a, at the fixed refractive index n corresponding to a wave incident along the optical axis, two different two-partial combinations can be realized. These differ by the choice of one reflected wave from the two possible waves that belong to different refraction sheets and that have different propagation directions and polarizations. This requires only properly choosing the polarization of the wave incident along the optical axis.

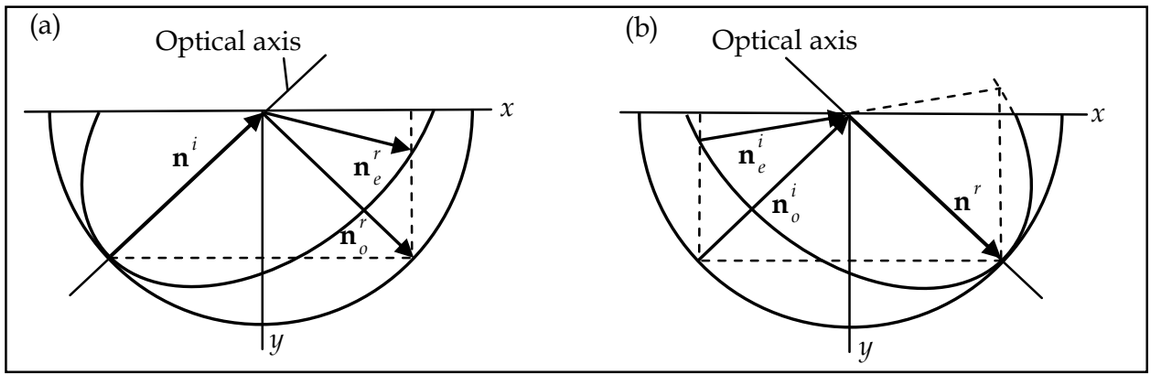

Fig. 6. Two-partial reflections in the $c_3 = 0$ plane when the incident (a) and reflected (b) waves coincide with the optical axis

In such degenerate directions, a crystal is known to allow the propagation of waves with a polarization arbitrarily oriented in the plane orthogonal to the optical axis. In particular, a wave with a polarization different from the two possible values corresponding to the two-partial reflections mentioned above can also be thrown on the surface in this direction. In this case, an ordinary three-partial reflection is realized in the crystal.

Any of the two possible incident waves corresponding to the same factor n (83) can also accompany the wave reflected along the optical axis (Fig. 6b). In this case, the crystal itself will choose such a polarization of the reflected degenerate wave that the total superposition of the two-partial reflection satisfies the boundary condition (19).

Clearly, four different two-partial reflections can be obtained at certain small perturbations of the reflection geometry shown in Fig. 6: two simple, $o \to o$ and $e \to e$, and two conversion, $o \to e$ and $e \to o$, ones. This ultimately resolves the paradox of the surprising coexistence of simple and conversion reflections in the $c_3 = 0$ plane.

The $c_2 = 0$ section ($\theta = 0$). In the $c_2 = 0$ coordinate plane, Eqs. (66) and (67) again coincide:

$$p_o(p_o^2 + c_3^2) = 0 \,. \tag{85}$$

Equation (85) has only one solution, $p_o = 0$, i.e.,

$$n = \hat{n}_o = \sqrt{\varepsilon_o} \,, \tag{86}$$

which corresponds to the one-partial ordinary eigenmode (54). At $\gamma > 1$, circumference (86) is the boundary of region I (37). We previously obtained the exceptional bulk polariton (54) by passing to the limit of grazing incidence, $n \to \hat{n}_o$, on the family of pure reflections. At the reverse perturbation of the refractive index, $n \leftarrow \hat{n}_o$, with the optical axis retained in the $c_2 = 0$ plane, polariton (54) naturally again splits into the two-partial solution corresponding to a pure reflection. However, at certain matched changes of the optical-axis orientation and the refractive index n corresponding to the motion along the conversion surface, the same ordinary polariton, being slightly distorted, will attach an extraordinary (incident or reflected) component with a small amplitude, which relates to a mode conversion.
In an optically negative crystal ($\gamma < 1$), circumference (86) lies outside region I (37), except for its two points at the intersection with the x axis (where the "mushroom cap" in Fig. 4b touches the "ground"). In the latter case, we are talking about the bulk polariton propagating along the optical axis parallel to x and characterized by parameters (59). The same points are also seen on the $c_3 = 0$ section (see Fig. 5b).

5. Resonance reflection from the metal coating with nonzero impedance

In this section we turn to a more practical problem considering wave reflections in a crystal from the metal coating which is not perfect anymore. The impedance of the metal will be supposed finite ($\zeta \neq 0$) but small. We shall consider the physical consequences of this new feature of the boundary problem on the example of rather nontrivial resonance of reflection which may be interpreted as an excitation of strong polariton by means of a weak incident pump wave. The idea of the resonance was already discussed in the Introduction. Now we are prepared to start a new stage of studies, following to (Depine & Gigli, 1995; Alshits & Lyubimov, 2010).
In this section, we consider in detail the specific features of resonance excitation of an extraordinary polariton in an optically negative crystal and of the accompanying plasmon in a metal by an incident ordinary pump wave. Similar results for an optically positive crystal will be shortly presented separately.

5.1 The structure of wave fields in a crystal

As we have seen, in crystals covered by a perfect metal there are two special geometries admitting simple reflections. They occur in the both sheets of the refraction surface when the optical axis is parallel to either the interface ($c_2 = 0$) or the sagittal plane ($c_3 = 0$). At grazing incidence simple reflections may transform into exceptional bulk waves: the ordinary wave - in the $c_2 = 0$ plane and the extraordinary wave – in the $c_3 = 0$ plane. In optically negative crystals ($\gamma < 1$) the extraordinary exceptional wave (56)-(58) belongs to an internal sheet of the refraction surface and is accompanied by the independent simple reflection of the ordinary waves at the same refractive index $n = \hat{n}_e^0$ (Fig. 7a). The wave characteristics of this simple reflection in accordance with Eqs. (49)-(51) are given by

$$\mathbf{n}_o^{0i,r} = (1,\ \mp\hat{p}_o^0,\ 0)\hat{n}_e^0, \qquad \hat{p}_o^0 = |c_2|(\hat{n}_o / \hat{n}_e^0)\sqrt{1-\gamma}, \tag{87}$$

$$\begin{pmatrix} \mathbf{e}_o^{0i,r} \\ \mathbf{h}_o^{0i,r} \end{pmatrix} = \begin{pmatrix} (0,\ 0,\ 1) \\ (\mp\hat{p}_o^0,\ -1,\ 0)\hat{n}_e^0 \end{pmatrix}, \qquad C_o^r = C_o^i. \tag{88}$$

Here we stress that in the $c_3 = 0$ plane these independent solutions also coexist even at $\zeta \neq 0$. That follows from Eqs. (33), (34) providing simple reflections in both wave branches ($D_{eo} = D_{oe} = 0$) in any symmetry plane ($c_3 = 0$) containing the optical axis. One of them at grazing incidence creates an extraordinary bulk polariton. Below we consider the mechanism of its excitation by means of a resonance reflection in the vicinity of this exceptional orientation.

Assuming that $\zeta \neq 0$, let us deviate the plane of incidence from the direction of the optical axis **c** by a small angle θ. Naturally this leads to a change in the orientation of the surface and in the coordinate system connected to the geometry, in which now

$$\mathbf{c} = (c_1,\ c_2,\ \hat{c}_3)^T\ , \tag{89}$$

where $\hat{c}_3 = \sin\theta$ (an arc over the parameter indicates that this parameter is small: $|\hat{c}_3| << 1$). When $\hat{c}_3 \neq 0$, the section of the refraction surface by the new plane of incidence xy (Fig. 7b) does not show any tangency of sheets, in contrast to the unperturbed situation of Fig. 7a.

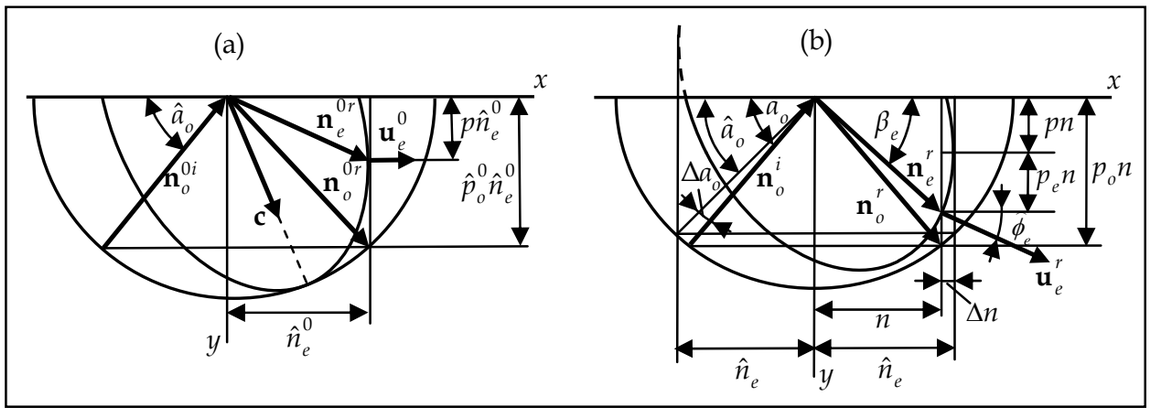

Fig. 7. The wave characteristics of reflections in an optically negative crystal; (a) in the absence of perturbation, $c_3 = 0$, and (b) with perturbation $c_3 \neq 0$. The refraction vectors are shown together with the sections of the refraction sheets by the plane of incidence xy

A perturbed expression for the limiting parameter $\hat{n}_e$ is given by the exact formula (35). This parameter corresponds to the perturbed limiting refraction vector

$$\hat{\mathbf{n}}_o^i = (1,\ -\hat{p}_o,\ 0)\hat{n}_e\ . \tag{90}$$

By varying the propagation direction of the incident ordinary wave with the refraction vector $\mathbf{n}_o^i$ near the limiting vector (90), we can conveniently represent the vector $\mathbf{n}_o^i$ as

$$\mathbf{n}_o^i = (1,\ -p_o,\ 0)n\ ,\quad p_o = \hat{p}_o + \Delta p_o\ ,\quad n = \hat{n}_e + \Delta n\ . \tag{91}$$

In other words, the angle of incidence $a_o = \arctan p_o$ (see Fig. 7b) of this wave becomes a free parameter close to the limiting angle $\hat{a}_o = \arctan\hat{p}_o$, where $\hat{p}_o = \sqrt{B/A - 1}$. Taking into account (11), one can easily find for ordinary waves the following relation

$$\Delta p_o \approx -[\varepsilon_o / (\hat{n}_e^0)^3]\Delta n\ , \tag{92}$$

which gives a relationship between Δn and $\Delta a_o = a_o - \hat{a}_o$:

$$\Delta n \approx -\hat{n}_e^0 \hat{p}_o^0 \Delta a_o \,, \tag{93}$$

where $\hat{n}_e^0$ and $\hat{p}_o^0$ are unperturbed limiting parameters defined by (58) and (87).
The wave field structure of the reflection is determined by the superposition of three partial waves given by Eqs. (4)-(7) with $C_e^i = 0$. A concretization of the parameter p_o in these formulae yields the expression

$$p_o \approx \hat{p}_o + \frac{\varepsilon_o}{(\hat{n}_e^0)^2} \Delta a_o \,, \tag{94}$$

p is defined by the exact Eq. (11) and the parameter p_e is determined by Eq. (36):

$$p_e = p_e(\Delta a_o) = \sqrt{\frac{\varepsilon_o \varepsilon_e}{(\hat{n}_e^0)^2}\left(\frac{1}{n^2} - \frac{1}{\hat{n}_e^2}\right)} \approx \frac{\sqrt{2\hat{p}_o^0 \varepsilon_o \varepsilon_e}}{(\hat{n}_e^0)^2} \begin{cases} \sqrt{\Delta a_o}\,, & \Delta a_o \geq 0, \\ i\sqrt{-\Delta a_o}\,, & \Delta a_o < 0. \end{cases} \tag{95}$$

As expected, the variation of the angle of incidence near the limiting position $\hat{a}_o$ leads to the transformation of the extraordinary partial wave from bulk reflected for $\Delta a_o \geq 0$ to the accompanying localized wave for $\Delta a_o < 0$. However, for sufficiently small $|\Delta a_o|$ in (31), when $|p_e| << 1$, in the first case we have nearly grazing refection, whereas, in the second case, the localized mode should be a deeply penetrating (quasibulk) wave. Thus, in either case the extraordinary wave remains a weakly perturbed initial bulk polariton (56).

5.2 Reflection coefficients and the excitation factor of a polariton-plasmon

An analysis of the considered resonance may be done basing on general solution (30)-(34) of the reflection problem specifying it to a small region of geometrical parameters $|\Delta a_o| << 1$, $\hat{c}_3^2 / c_2^2 << 1$ and limiting ourselves to the linear approximation in the impedance ζ. In this case one can replace in (32)-(34) $R \to 1$ retaining only terms $\sim \zeta$. The results are

$$r_{eo}(\delta, \Delta a_o) \equiv \frac{C_e^r}{C_o^i} = -\frac{\delta \kappa_o \gamma \hat{n}_o}{\delta^2 \kappa_o \hat{n}_e^0 / 2 + \sqrt{\kappa_o \gamma \Delta a_o} + \zeta} \,, \tag{96}$$

$$r_{oo}(\delta^2, \Delta a_o) \equiv \frac{C_o^r}{C_o^i} = \frac{\delta^2 \kappa_o \hat{n}_e^0 / 2 - \sqrt{\kappa_o \gamma \Delta a_o} - \zeta}{\delta^2 \kappa_o \hat{n}_e^0 / 2 + \sqrt{\kappa_o \gamma \Delta a_o} + \zeta} \,, \tag{97}$$

where the notation is introduced

$$\kappa_o = 2\hat{p}_o^0 (\hat{n}_e^0 / \varepsilon_e)^2 \,, \qquad \delta = \hat{c}_3 / c_2 \,. \tag{98}$$

Eqs. (96), (97) are valid for either sign of Δa_o; however one should remember that at the change of this sign all square roots in these equations become imaginary instead of real, or vise versa, as in (95). Below we will see that the reflection coefficients exhibit completely different behavior in the domains with real and imaginary parameter p_e.
Both the numerators and denominators in the functions (96) and (97) are combinations of small quantities, and even a small variation of these quantities may lead to large variations

of the functions themselves. It is this fact that is responsible for the resonance properties of the reflection: a sharp increase or, conversely, decrease in the relative intensity of the partial components in the related wave superposition for appropriate combinations of the small parameters Δa_o, δ, and ζ.

As the measure of efficiency of a resonance, introduce the excitation factor of an extraordinary polariton as the ratio of the moduli of Poynting vectors:

$$K_{eo} = \left|\mathbf{P}_e^r\right| / \left|\mathbf{P}_o^i\right|_{y=0} . \tag{99}$$

The energy fluxes $\mathbf{P}_o^i$ and $\mathbf{P}_o^r$ entering (99) are related to the energy densities w_o^i and w_e^r of the corresponding waves by the formulas

$$|\mathbf{P}_o^i| = w_o^i |\mathbf{u}_o^i| = w_o^i c / \hat{n}_o, \quad |\mathbf{P}_e^r| = w_e^r |\mathbf{u}_e^r| = w_e^r c / \hat{n}_e^0 . \tag{100}$$

Here $\mathbf{u}_o^i$ and $\mathbf{u}_e^r$ are the group velocities (3), which can be calculated near the peak in zero approximation; moreover, by definition we have

$$w_o^i = \frac{1}{8\pi}|\mathbf{H}_o^i|^2 = \frac{1}{8\pi}|\mathbf{h}_o^i C_o^i|^2 = \frac{1}{8\pi}|C_o^i|^2, \quad w_e^r = \frac{1}{8\pi}|C_e^r|^2 . \tag{101}$$

Taking into account these relations and Eq. (96), we obtain

$$K_{eo}(\delta^2, \Delta a_o) = \frac{\hat{n}_o}{\hat{n}_e^0}\left|r_{eo}(\delta, \Delta a_o)\right|^2 . \tag{102}$$

Figure 8 shows a three-dimensional picture of the maximum of the excitation factor $K_{eo}(\delta^2, \Delta a_o)$ of an extraordinary polariton and the minimum of $|r_{oo}(\delta^2, \Delta a_o)|^2$ for the same combination of the control parameters δ^2 and Δa_o for a sodium nitrate crystal with aluminum coating at a wavelength in vacuum of λ_0 = 0.85 μm. Below, these characteristics of the resonance will be studied in more detail.

Let us show that the factor $K_{eo}(\delta^2, \Delta a_o)$ simultaneously characterizes the excitation of the accompanying surface plasmon in the metal (y < 0), whose field is given by Eqs. (8), (9). In zero approximation (when c_3 = 0 and ζ = 0), the polarization of the excited extraordinary polariton (56), (57) is close to the *TM* type, while the polarizations of the incident and reflected ordinary waves $(50)_1$, to the *TE* type. In this case, the ratio of the amplitudes of these components at resonance, which is characterized by the excitation factor K_{eo}, shows that the dominant polarization of the whole wave superposition is the *TM* polarization, when the field **H** is parallel to the z axis. Since the tangential components $\mathbf{H}_t$ must be continuous on the interface (Landau & Lifshitz, 1993), the plasmon amplitudes can be estimated as $C_{TM} \approx C_e$ and $|C_{TE}| << |C_{TM}|$. Taking into account these relations and the normalization condition $|\mathbf{h}_{TM}| = |\mathbf{h}_e| = 1$, we obtain the following expression in zero approximation:

$$|C_{TM} / C_o^i|^2 \approx |C_e / C_o^i|^2 = |r_{eo}(\delta, \Delta a_o)|^2 . \tag{103}$$

Thus, the factor K_{eo} (102) describes the resonance excitation of both a polariton in the crystal and a localized plasmon in the metal coating.

5.3 Resonance excitation of a surface polariton

When the pumping ordinary wave is incident on the crystal boundary at angle $a_o < \hat{a}_o$, an extraordinary surface polariton is excited. In this case formulas (96) and (102) yield

$$K_{eo}(\delta^2, \Delta a_o) = \frac{(\delta\kappa_o\varepsilon_e)^2 / n_o\hat{n}_e^0}{\left(\delta^2\kappa_o\hat{n}_e^0 / 2 + \zeta'\right)^2 + \left(\sqrt{-\kappa_o\gamma\Delta a_o} - |\zeta''|\right)^2}. \quad (104)$$

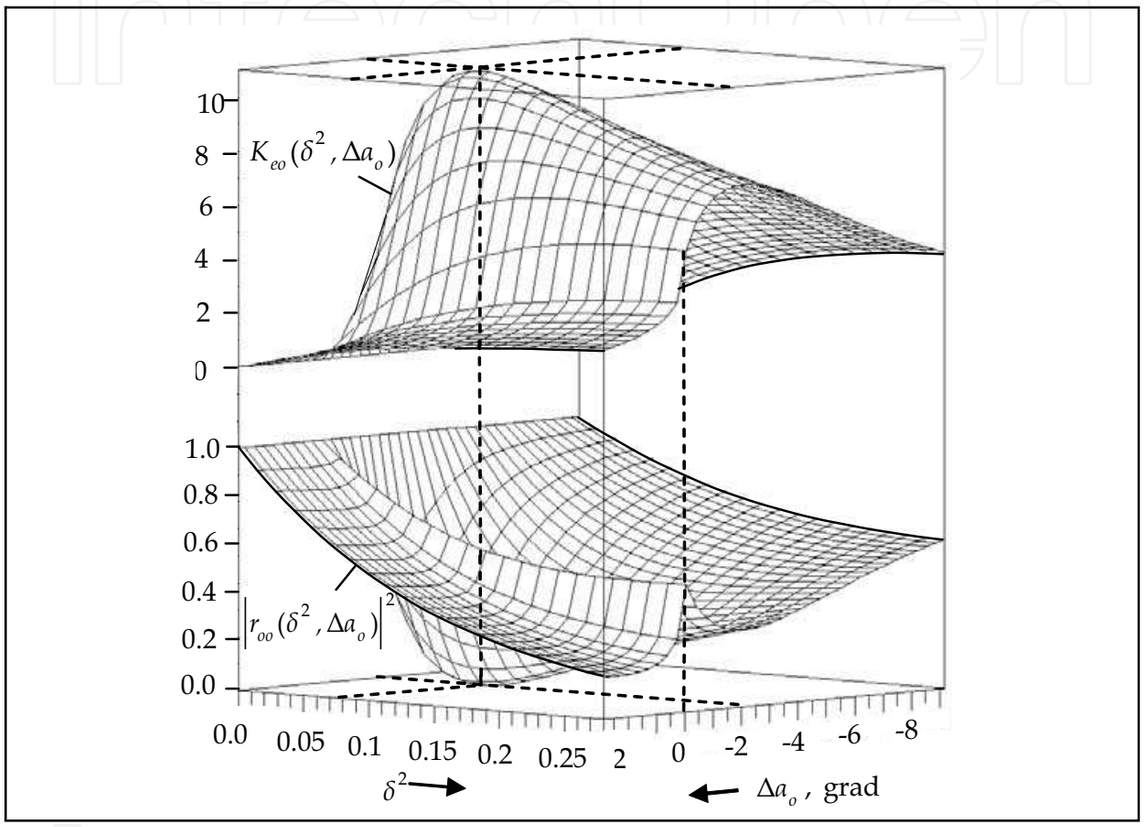

Fig. 8. Surfaces (a) $K_{eo}(\delta^2, \Delta a_o)$ and (b) $|\, r_{oo}(\delta^2, \Delta a_o)\,|^2$ for a sodium nitrate crystal with aluminum coating for λ_0 = 0.85 μm.

As a function of the deviation of the incidence angle Δa_o, this expression has an obvious maximum for

$$\Delta a_o^{max} = -|\zeta''|^2 / \kappa_o\gamma. \quad (105)$$

For a fixed value of $\Delta a_o = \Delta a_o^{max}$, the excitation factor remains a function of the value δ^2:

$$K_{eo}\left(\delta^2, \Delta a_o^{max}\right) = \frac{(\delta\kappa_o\varepsilon_e)^2 / n_o\hat{n}_e^0}{\left(\delta^2\kappa_o\hat{n}_e^0 / 2 + \zeta'\right)^2}, \quad (106)$$

which also has a maximum for an appropriate choice of $\delta \equiv \hat{c}_3 / c_2$:

$$\delta^2_{max} = 2\zeta' / \kappa_o \hat{n}^0_e \,. \tag{107}$$

Substituting (107) into (106), we find the absolute maximum of the excitation factor

$$K^{max}_{eo} = K_{eo}\left(\delta^2_{max}, \Delta a^{max}_o\right) = \frac{\kappa_o \gamma \varepsilon_e \hat{n}_o}{2(\hat{n}^0_e)^2 \zeta'} = \frac{\hat{p}^0_o}{n_o \zeta'} \tag{108}$$

which is inversely proportional to the small parameter ζ'; this guarantees the efficiency of the resonance, especially in the infrared region. According to (87) and (58), the numerator in (108) is expressed as

$$\hat{p}^0_o = \frac{|c_2|\sqrt{1-\gamma}}{\sqrt{1-(1-\gamma)c_2^2}} \,. \tag{109}$$

This shows that the coefficient K^{max}_{eo} can be additionally increased by choosing a crystal with high anisotropy factor $(1-\gamma)$ and the orientation of the optical axis in the yz plane ($c_1 = 0$) corresponding to the maximum possible component $|c_2| = 1$. As a result, we obtain $\hat{p}^0_o = \sqrt{1/\gamma - 1}$ and, instead of (108), we have the optimized value

$$K^{max}_{eo} = \frac{1}{\zeta'}\sqrt{\frac{\varepsilon_o - \varepsilon_e}{\varepsilon_o \varepsilon_e}} \,. \tag{110}$$

Below we will assume that $c_1 = 0$ in all numerical estimates and figures.
In terms of the ratios K_{eo} / K^{max}_{eo}, $\delta^2 / \delta^2_{max}$, and $\Delta a_o / \Delta a^{max}_o$, the sections of the peak (104) for a fixed value of the parameter $\Delta a_o = \Delta a^{max}_o$ (105) or $\delta^2 = \delta^2_{max}$ (107) are given by

$$K_{eo}\left(\delta^2, \Delta a^{max}_o\right) = \frac{4\delta^2 / \delta^2_{max}}{(\delta^2 / \delta^2_{max} + 1)^2} K^{max}_{eo} \,, \quad K_{eo}(\delta^2_{max}, \Delta a_o) = \frac{K^{max}_{eo}}{\left(\dfrac{\sqrt{\Delta a_o / \Delta a^{max}_o} - 1}{2\zeta' / \zeta''}\right)^2 + 1} \,. \tag{111}$$

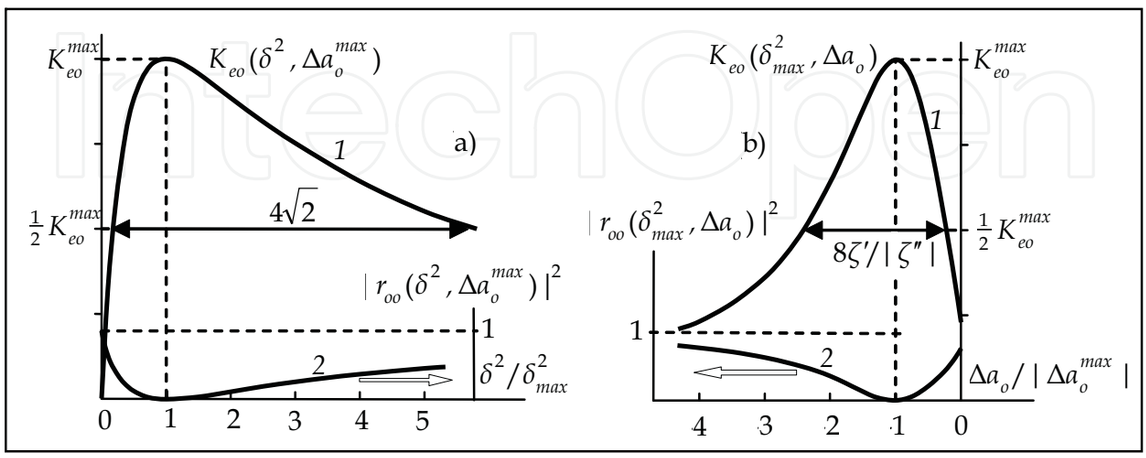

Fig. 9. Two sections of the surfaces $K_{eo}(\delta^2, \Delta a_o)$ and $|r_{oo}(\delta^2, \Delta a_o)|^2$ shown in Fig. 8 when (a) $\Delta a_o \equiv \Delta a^{max}_o \approx$ --2.1 or (b) $\delta^2 \equiv \delta^2_{max} \approx 0.078$; λ_0 = 0.85 μm and $K^{max}_{eo} \approx 10.8$

Figure 9a (curve *1*) shows that the section of the peak for $\Delta a_o = \Delta a_o^{max}$ rapidly reaches a maximum and then slowly decreases as the parameter δ increases. Of course, this is advantageous for applications but restricts (at least, in the visible range) the applicability of the approximation based on the inequality $\delta^2 << 1$. The half-width of this peak is

$$(\Delta\delta^2)_{1/2} = 4\sqrt{2}\delta_{max}^2 = 8\sqrt{2}\zeta' / \kappa_o \hat{n}_e^0 . \tag{112}$$

Away from the section $\Delta a_o = \Delta a_o^{max}$, the coordinate of the maximum and the half-width of the peak with respect to δ noticeably increase, which is clearly shown in the three-dimensional picture of the peak in Fig. 8.

Another section of the same peak (for $\delta^2 = \delta_{max}^2$) is shown in Fig. 9b (curve *1*). According to $(111)_2$, its half-width is

$$(\Delta\alpha_o)_{1/2} = \frac{8\zeta'}{|\zeta''|} |\Delta\alpha_o^{\max}| = \frac{8\zeta' |\zeta''|}{\kappa_o \gamma} . \tag{113}$$

Compared with (112), this quantity contains an additional small parameter $|\zeta''|$, which accounts for the relatively small width in this section of the peak in the region $|\Delta a_o| << 1$.

The penetration depth d_e of a polariton into a crystal is limited by the parameter p_e and, according to (95), depends on the angle Δa_o. At the maximum point $\Delta a_o = \Delta a_o^{max}$ (105), the penetration depth is

$$d_e = \frac{1}{k \operatorname{Im} p_e} \approx \frac{1}{k_0 \hat{n}_e^0 \operatorname{Im} p_e} = \frac{\lambda_0 (\hat{n}_e^0)^2}{2\pi\varepsilon_o \varepsilon_e |\zeta''|} . \tag{114}$$

The plasmon penetration depth into the metal is found quite similarly

$$d_m = \frac{1}{k \operatorname{Im} p_m} \approx \frac{\lambda_0 |\zeta''|}{2\pi} , \tag{115}$$

where we have made use of Eq. $(11)_4$ by expressing $\operatorname{Im} p_m \approx 1/|\zeta''| \hat{n}_e^0$. Comparing Eqs. (114) and (115), we can see that the plasmon in metal is localized much stronger than the polariton in the crystal: $d_m / d_e \sim |\zeta''|^2$.

In Fig. 9, the material characteristics of the crystal ε_o and ε_e, as well as the geometric parameters c_1 and c_2 are "hidden" in the normalizing factors δ_{max}^2, Δa_o^{max}, and K_{eo}^{max}. The first section (Fig. 9a) is independent of other parameters and represents a universal characteristic in a wide range of wavelengths, whereas the second section (Fig. 9b) depends on the ratio $\zeta'/|\zeta''|$ obtained from Table 1 for aluminum at a vacuum wavelength of λ_0 = 0.85 μm.

λ_0, μm	0.4	0.5	0.6	0.85	1.2	2.5	5.0
ζ'	0.0229	0.0234	0.0253	0.0373	0.0092	0.0060	0.0046
$-\zeta''$	0.267	0.215	0.180	0.135	0.108	0.050	0.026

Table 1. Components of the surface impedance $\zeta = \zeta' + i\zeta''$ for aluminum in the visible and infrared ranges at room temperature, obtained from the data of (Motulevich, 1969)

The absolute values of the main parameters of the peak are shown in Table 2 for a sodium nitrate crystal $NaNO_3$ for various wavelengths. In our calculations (including those related to Fig. 8), we neglected a not too essential dispersion of permittivities and used fixed values of $\varepsilon_o = 2.515$, $\varepsilon_e = 1.785$, and $\gamma = 0.711$ (Sirotin & Shaskolskaya, 1979, 1982) at $\lambda_0 = 0.589$ μm. First of all, it is worth noting that, in the visible range of wavelengths of $\lambda_0 = 0.4$--0.6 μm, the maximal excitation factor (110) relatively slowly decreases as λ_0 increases, although remains rather large ($K_{eo}^{max} \approx 16$--18). With a further increase in the wavelength to the infrared region of the spectrum, the factor first continues to decrease down to a point of $\lambda_0 = 0.85$ μm and then rather rapidly increases and reaches a value of about 90 at $\lambda_0 = 5$ μm. The half-width of the peak $(\Delta a_o)_{1/2}$ (113), starting from the value of $(\Delta a_o)_{1/2} \approx 5°$, rapidly decreases as the wavelength increases and becomes as small as about 0.1° at $\lambda_0 = 5$ μm, which, however, is greater than the usual angular widths of laser beams. The half- width $(\Delta\delta^2)_{1/2}$ (112) differs from δ_{max}^2 (107) only by a numerical factor of $4\sqrt{2}$ and therefore is not presented in the table. The penetration depth d_e (114) of a polariton into the crystal at the point of absolute maximum of the resonance peak is comparable with the wavelength of the polariton and remains small even in the infrared region, although being much greater than the localization depth d_m of the plasmon (115). However, as $\Delta a_o \to 0$, $p_e \to 0$ (95), the penetration depth d_e rapidly increases, and the polariton becomes a quasibulk wave. The optimized perturbation $\delta_{\max}$ corresponding to the angle $\theta_{\max} = \arctan\delta_{\max}$ remains small over the entire range of wavelengths and varies from 0.05 to 0.01, which certainly guarantees the correctness of the approximate formulas obtained.

	λ_0, μm	0.4	0.6	0.85	1.2	2.5	5.0
Surface polariton (a pumped mode) $\Delta a_o^{max} < 0$	K_{eo}^{max}	17.6	15.9	10.8	43.8	67.1	87.5
	$(\Delta a_o)_{1/2}$	5.5°	4.1°	4.5°	0.9°	0.3°	0.11°
	d_e, μm	0.090	0.225	0.399	0.719	3.18	12.4
	$-\Delta a_o^{max}$	8.0°	3.6°	2.1°	1.3°	0.3°	0.08°
	δ_{max}^2	0.048	0.053	0.078	0.019	0.013	0.010
	θ_{max}	12°	13°	16°	7.8°	6.5°	5.7°
	ψ_o	15°	15°	18°	9.3°	7.7°	6.8°
Bulk polariton $\Delta a_o^{max} = 0$	$\overline{K}_{eo}^{max}$	2.7	3.9	4.6	6.9	14.4	26.3
	$\overline{\delta}_{max}^2$	0.56	0.38	0.28	0.23	0.11	0.05
	$\overline{\theta}_{max}$	37°	32°	28°	26°	18°	13°
Plasmon	d_m, μm	0.017	0.017	0.018	0.021	0.020	0.021

Table 2. Parameters of polaritons excited in an optically negative sodium nitrate crystal with aluminum coating for various wavelengths ($c_1 = 0$, $\hat{a}_o = 32.5°$)

5.4. Conversion reflection and a pumped surface mode

Now we consider the reflection coefficient (97) in more detail for $\Delta a_o < 0$:

$$r_{oo}(\delta^2, \Delta a_o) \equiv \frac{C_o^r}{C_o^i} = \frac{\delta^2 \kappa_o \hat{n}_e^0 / 2 - \zeta' - i\left(\sqrt{-\kappa_o \gamma \Delta a_o} - |\zeta''|\right)}{\delta^2 \kappa_o \hat{n}_e^0 / 2 + \zeta' + i\left(\sqrt{-\kappa_o \gamma \Delta a_o} - |\zeta''|\right)}. \tag{116}$$

In contrast to the excitation factor K_{eo} (104) of the extraordinary polariton, the reflection coefficient (116) does not "promise" any amplification peaks. Conversely, it follows from (116) that the amplitude of the ordinary reflected wave never exceeds in absolute value the amplitude of the incident wave. Moreover, the substitution of the coordinates Δa_o^{max} (105) and δ_{max} (107) of the absolute maximum of the excitation factor (104) into (116) gives the absolute minimum (see Fig. 8 and curves *2* in Fig. 9):

$$|r_{oo}(\delta_{max}^2, \Delta a_o^{max})|^2 = 0 \tag{117}$$

Thus, the resonance reflection in the optimized geometry is a conversion reflection (i.e., a two-partial reflection with a change of branch) and a quite nontrivial one at that. Indeed, in this case the incident ordinary partial wave in the crystal is accompanied by a unique wave, which, being an extraordinary wave belongs to the other refraction sheet and is not a bulk reflected wave. This wave is localized at the interface between the crystal and metal and transfers energy along the interface (Fig. 10).

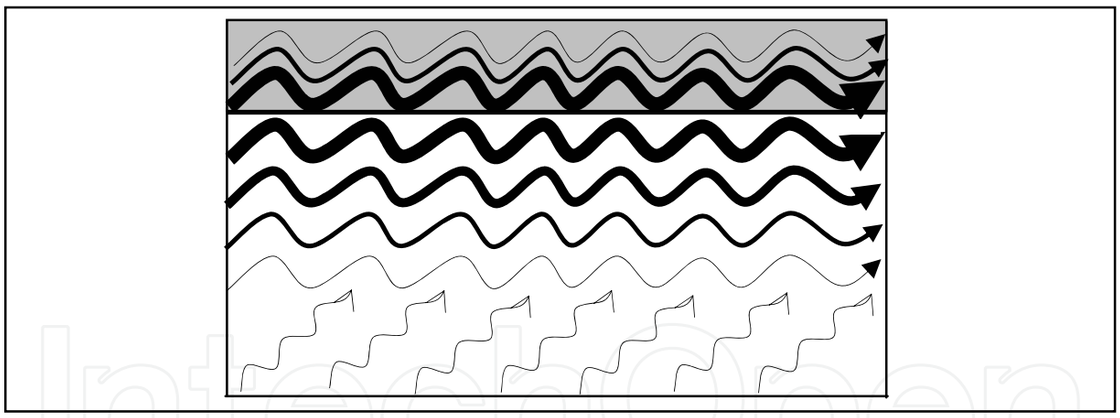

Fig. 10. Schematic picture of the pumped polariton-plasmon near the interface between a crystal and metal coating

Naturally, in this case the absence of the reflected wave does not imply the violation of the energy conservation law; just the propagation geometry corresponding to the minimum (117) is chosen so that the normal component of the Poynting vector of the incident wave is completely absorbed in the metal. This component is estimated by means of $(100)_1$:

$$|\mathbf{P}_{o\perp}^i| = |\mathbf{P}_o^i| \sin a_o = w_o^i (c / \hat{n}_o) \hat{p}_o^0 (\hat{n}_e^0 / \hat{n}_o) = c w_o^i \hat{p}_o^0 \hat{n}_e^0 / \varepsilon_o . \tag{118}$$

Following (Landau & Lifshitz, 1993) and relations (100), (101), and (103), we can easily verify that this component is equal the normal energy flux absorbed by the metal coating at resonance:

$$|\mathbf{P}_{m\perp}| = \frac{c\zeta'}{8\pi}|\mathbf{H}_t|_S^2 = c\zeta'|r_{eo}|_{max}^2 w_o^i = cw_o^i \frac{\hat{p}_o^0 \hat{n}_e^0}{\varepsilon_o}. \quad (119)$$

It is not incidental that the final expression for $|\mathbf{P}_{m\perp}|$ does not contain the components of the impedance. Indeed, according to the energy conservation law, in this case dissipation should completely compensate the normal energy flux in the incident wave, which "knows" nothing about the metallization of the crystal surface. It is essential that the dissipation (119), remaining comparable with the energy flux density in the incident wave, is very small compared with the intensity of the polariton--plasmon localized at the interface:

$$|\mathbf{P}_e|_{max} = w_e|_S \frac{c}{\hat{n}_e^0} = \frac{1}{8\pi}|\mathbf{H}_e|_S^2 \frac{c}{\hat{n}_e^0} = |r_{eo}|_{max}^2 \frac{cw_o^i}{\hat{n}_e^0} >> |\mathbf{P}_{m\perp}|. \quad (120)$$

The fact that the energy flux of the polariton--plasmon at the interface is considerably greater than the intensity of the pumping wave in no way contradicts either the energy conservation law or the common sense. We consider a steady-state problem on the propagation of infinitely long plane waves. In this statement, the superposition of waves jointly transfers energy along the surface from --∞ to +∞. These waves exist only together, and the question of the redistribution of energy between the partial waves can be solved only within a non-stationary approach. Indeed, suppose that, starting from a certain instant, a plane wave coinciding with our ordinary wave is incident on the surface of a crystal. Upon reaching the boundary, this wave generates an extraordinary wave whose amplitude increases in time and gradually reaches a steady-state regime that we describe. Naturally, the time of reaching this regime is the larger, the higher the peak of the excitation factor.

In fact, the conversion reflection considered represents an eigenwave mode that arises due to the anisotropy of the crystal. It is natural to call this mode, consisting of a surface polariton--plasmon and a weak pumping bulk wave, a *pumped* surface wave by analogy with the known *leaky* surface waves, which are known in optics and acoustics (Alshits et al., 1999, 2001). The latter waves also consist of a surface wave and the accompanying weak bulk wave, which, in contrast to our case, removes energy from the surface to infinity, rather than brings it to the surface; i.e., it is a leak, rather than a pump, partial wave.

Numerical analysis of the exact expression for the reflection coefficient r_{oo}, Eqs. $(30)_1$, (32), has shown (Lyubimov et al., 2010) that the conversion phenomenon (117) retains independently of the magnitude of the impedance ζ. However it turns out that for not too small ζ, positions of the maximum of the excitation factor K_{eo} and the minimum (117) of the reflection coefficient r_{oo} do not exactly coincide anymore, as they do in our approximation.

5.5. Resonance excitation of a bulk polariton

When a pump wave of the ordinary branch is incident at angle $a_o \geq \hat{a}_o$ on the boundary of the crystal, a bulk extraordinary polariton is generated. The expression, following from (96) and (102), for the excitation factor K_{eo} of such a polariton is significantly different from expression (104), which is valid for $\Delta a_o < 0$:

$$K_{eo}(\delta^2, \Delta a_o) = \frac{(\delta\kappa_o\varepsilon_e)^2 / \hat{n}_o\hat{n}_e^0}{\left(\delta^2\kappa_o\hat{n}_e^0/2 + \sqrt{\kappa_o\gamma\Delta a_o} + \zeta'\right)^2 + \zeta''^2}. \quad (121)$$

As the angle Δa_o increases, the function (121) monotonically decreases, so that the excitation factor attains its maximum for $\Delta a_o = 0$, i.e., for $a_o = \hat{a}_o$:

$$K_{eo}(\delta^2, 0) = \frac{(\delta\kappa_o\varepsilon_e)^2 / \hat{n}_o\hat{n}_e^0}{\left(\delta^2\kappa_o\hat{n}_e^0 / 2 + \zeta'\right)^2 + \zeta''^2}. \tag{122}$$

In turn, formula (122), as a function of the parameter δ^2, forms a peak with the coordinate of the maximum

$$\bar{\delta}^2_{max} = \frac{2|\zeta|}{\kappa_o\hat{n}_e^0} \approx \frac{2|\zeta''|}{\kappa_o\hat{n}_e^0}. \tag{123}$$

Note that the optimized parameters $\bar{\delta}^2_{max}$ (123) and δ^2_{max} (107) for the excitation of bulk and localized polaritons are substantially different (see Table 1):

$$\bar{\delta}^2_{max} / \delta^2_{max} \approx |\zeta''| / \zeta'. \tag{124}$$

With regard to (123), the absolute maximum of the excitation factor (121) is expressed as

$$\bar{K}_{eo}^{max} = K_{eo}(\bar{\delta}^2_{max}, 0) = \frac{2\hat{p}_o^0}{\hat{n}_o\left(|\zeta| + \zeta'\right)} \approx \frac{2\hat{p}_o^0}{\hat{n}_o\left(|\zeta''| + \zeta'\right)}. \tag{125}$$

Next, by analogy with (110) and with regard to (109), for $c_1 = 0$ we obtain the following optimized value:

$$\bar{K}_{eo}^{max} \approx \frac{2}{|\zeta''| + \zeta'}\sqrt{\frac{\varepsilon_o - \varepsilon_e}{\varepsilon_o\varepsilon_e}}. \tag{126}$$

The approximate equality in formulas (123)--(126) implies that the terms of order $\sim (\zeta' / \zeta'')^2 << 1$ are omitted.

The three-dimensional picture of the excitation peak (121) is shown in Fig. 8 as a slope of a ridge in the region $\Delta a_o \geq 0$. The figure shows that, in the domain $\delta \sim \bar{\delta}_{max}$, $\Delta a_o \approx 0$, the factor $K_{eo}(\delta^2, \Delta a_o)$ rather weakly depends on δ and can be estimated at $\delta = \bar{\delta}_{max}$ as

$$K_{eo}(\bar{\delta}^2_{max}, \Delta a_o) \approx \frac{\bar{K}_{eo}^{max}}{1 + \sqrt{\Delta a_o / |\Delta a_o^{max}|}}. \tag{127}$$

The half-width of this one-sided peak is obviously given by $(\Delta a_o)_{1/2} = |\Delta a_o^{max}|$. In Fig. 8, the section (127) is shown as the edge of the surface $K_{eo}(\delta^2, \Delta a_o)$ that reaches the plane $\delta^2 = \bar{\delta}^2_{max} \approx 0.28$ (see Table 2).

Note that, in the domain $\Delta a_o \geq 0$, conversion is impossible ($r_{oo} \neq 0$) for $\zeta \neq 0$; thus, along with the extraordinary reflected wave, an ordinary reflected wave always exists, such that

$$|r_{oo}(\bar{\delta}^2_{max}, \Delta a_o)|^2 \approx \frac{1 - \sqrt{\Delta a_o / |\Delta a_o^{max}|} - \zeta' / |\zeta''|}{1 + \sqrt{\Delta a_o / |\Delta a_o^{max}|} + \zeta' / |\zeta''|}. \tag{128}$$

where, just as in (127), the terms quadratic in ζ' and linear in Δa_o are omitted. Formula (128) shows that, for $\Delta a_o << |\Delta a_o^{max}|$, $\zeta' << |\zeta''|$, the absolute values of the amplitudes of the incident and ordinary reflected waves are rather close to each other; hence, if we neglect the dissipation in the metal, nearly all the energy of the incident wave is passed to the ordinary reflected wave. In this situation, the presence of additional quite intense extraordinary reflected wave looks paradoxical.

This result can be more clearly interpreted in terms of wave beams rather than plane waves (Fig. 11). Let us take into consideration that plane waves are an idealization of rather wide (compared to the wavelength) beams of small divergence. Of course, it is senseless to choose the angle Δa_o smaller than the angle of natural divergence of a beam. However, this angle can be very small (10^{-4}--10^{-3} rad) for laser beams. If the width of an incident beam of an ordinary wave is l, then the reflected beam of the same branch of polarization has the same width. However, the beam of an extraordinary wave is reflected at a small angle $\hat{\varphi}_e$ to the surface, and its width $\hat{l}$ should also be small: $\hat{l} = \hat{\varphi}_e l / \sin a_o$ (Fig. 11). It can easily be shown that this width decreases so that even a small amount of energy in a narrow beam ensures a high intensity of this wave. The consideration would be quite similar to our analysis of the energy balance in the previous sub-section.

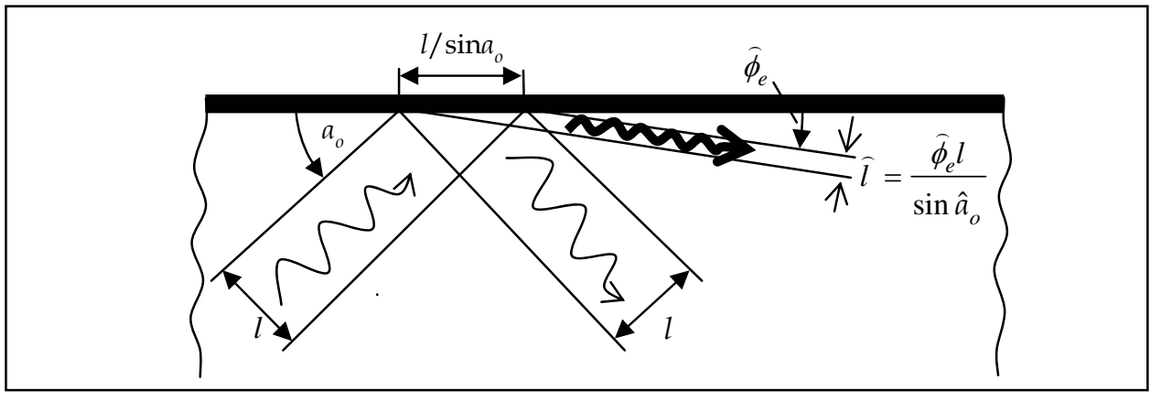

Fig. 11. The scheme of the resonance excitation of a bulk polariton by a finite-width beam

Fortunately, even a small deviation of Δa_o from zero easily provides a compromise that allows one, at the expense of the maximum possible intensity in the extraordinary reflected wave, to keep this intensity high enough and, moreover, to direct a significant part of the energy of the incident wave to this reflected wave. Indeed, formulas (127) and (128) show that, say, at $\Delta a_o \approx 0.1 |\Delta a_o^{max}|$, the energy is roughly halved between the reflected waves, and $K_{eo} \approx 0.76\, \overline{K}_{eo}^{max}$. For $\Delta a_o \approx 0.2 |\Delta a_o^{max}|$, we obtain $|r_{oo}|^2 \approx 0.3$ and $K_{eo} \approx 0.7\, \overline{K}_{eo}^{max}$.

The ratio of the absolute maxima (110) and (126) taken for different optimizing parameters δ_{max}^2 and $\overline{\delta}_{max}^2$, respectively, is usually much greater than unity:

$$\frac{K_{eo}(\delta_{max}^2, \Delta a_o^{max})}{K_{eo}(\overline{\delta}_{max}^2, 0)} = \frac{K_{eo}^{max}}{\overline{K}_{eo}^{max}} = \frac{1}{2}\left(\frac{|\zeta''|}{\zeta'} + 1\right). \tag{129}$$

In other words, the excitation efficiency of bulk polaritons is less than that of surface polaritons (see Table 2). Nevertheless, the attainable values of the excitation factor $\overline{K}_{eo}^{max}$ of a bulk polariton are in no way small. According to Table 2, when $\Delta a_o = 0$, the intensity of the

reflected extraordinary wave is three or four times greater than that of the incident ordinary wave even in the visible range of wavelengths of 0.4--0.6 μm (however, since the parameter $\overline{\delta}^2_{max}$ in this part of the table is not small enough, the accuracy of these estimates is low). Toward the infrared region, the surface impedance ζ of the aluminum coating decreases (see Table 1), while the excitation constant sharply increases, reaching values of tens.

5.6 Anormalous reflection of an extraordinary wave

Now we touch upon the specific features of the resonance excitation of an ordinary polariton by an incident extraordinary pumping wave. As mentioned above, such an excitation is possible only in optically positive crystals ($\gamma > 1$). The resonance arises under the perturbation of the geometry in which a bulk polariton of the ordinary branch (54) and simple reflection (44)-(46) in the extraordinary branch exist independently of each other.

Let us slightly "perturb" the orientation of the crystal surface by rotating it through a small angle $\theta = \arcsin\hat{c}_2$ with respect to the optical axis: **c** = (c_1, $\hat{c}_2$, c_3). The structure of the corresponding perturbed wave field is determined by formula (5) at $C^i_o = 0$ in which the appropriate vector amplitudes (6), (7) are substituted. The perturbed polarization vectors are found from formulas (14), (15), and the geometrical meaning of the parameters p, p_e, and p_o is illustrated in Fig. 2a. The refraction vectors, which determine the propagation direction of the incident and reflected waves, are present in (10). In the considered case the horizontal component n of the refraction vector is close to the limiting parameter $\hat{n}_o = \sqrt{\varepsilon_o}$ (Fig. 3), and the parameter p_e is close to the limiting value of $\hat{p}_e$: $n = \hat{n}_o + \Delta n$, $p_e = \hat{p}_e + \Delta p_e$. Here the parameter $\hat{p}_e$ is given by the exact expression $\hat{p}^2_e = (\gamma - 1)(A - c_1^2)/A^2$ and p is defined by Eq. (11) as before. The angle of incidence a_e of the extraordinary wave (Fig. 2a) is now close to the angle $\hat{a}_e = \arctan(\hat{p}_e - p)$: $a_e = \hat{a}_e + \Delta a_e$. The relation between the increments Δn, Δp_e, and Δa_e has the form

$$\Delta n = -\hat{p}^0_e n_o (c_1^2 / \gamma + c_3^2)\Delta a_e, \quad \Delta p_e = (c_1^2 + \gamma c_3^2)\Delta a_e, \tag{130}$$

where $\hat{p}^0_e$ relates to the unperturbed $c_2 = 0$: $\hat{p}^0_e = |c_3|\sqrt{\gamma - 1}$. Another important characteristic of the resonance is the angle of reflection β_o,

$$\beta_o = \arctan p_o, \qquad p_o \approx \sqrt{\varepsilon_o \kappa_e} \begin{cases} \sqrt{\Delta a_e}, & \Delta a_e \geq 0, \\ i\sqrt{-\Delta a_e}, & \Delta a_e < 0, \end{cases} \tag{131}$$

$$\kappa_e = 2\hat{p}^0_e (c_1^2 / \varepsilon_e + c_3^2 / \varepsilon_o). \tag{132}$$

Introduce a small parameter $\delta = \hat{c}_2 / c_3$, which is the inverse of $(98)_2$. Now, instead of (96) and (97), we have the following expressions for the reflection coefficients:

$$r_{oe}(\delta, \Delta a_e) \equiv \frac{C^r_o}{C^i_e} = \frac{2\hat{p}^0_e \delta / \sqrt{\varepsilon_e}}{\delta^2 \hat{p}^0_e / \hat{n}_o + \sqrt{\kappa_e \Delta a_e} + \zeta}, \tag{133}$$

$$r_{ee}(\delta^2, \Delta a_e) \equiv \frac{C^r_e}{C^i_e} = \frac{\delta^2 \hat{p}^0_e / \hat{n}_o - \sqrt{\kappa_e \Delta a_e} - \zeta}{\delta^2 \hat{p}^0_e / \hat{n}_o + \sqrt{\kappa_e \Delta a_e} + \zeta}. \tag{134}$$

These expressions exhibit the same structure of dependence on the small parameters δ and Δa_e as formulas (96) and (97) for optically negative crystals. Naturally, the main features of the reflection resonance considered above nearly completely persist under new conditions.
By analogy with (99), let us introduce the excitation factor of an ordinary polariton,

$$K_{oe}(\delta^2, \Delta a_e) = \left|\mathbf{P}_o^r\right| / \left|\mathbf{P}_e^i\right|_{y=0} = (|\mathbf{u}_o^r| / |\mathbf{u}_o^i|)\left|r_{oe}(\delta, \Delta a_e)\right|^2, \tag{135}$$

where $\mathbf{u}_o^r$ and $\mathbf{u}_e^i$ are the group velocities (3) of the excited and incident waves (in zero approximation): $|\mathbf{u}_o^r| = c / \hat{n}_o$, $|\mathbf{u}_e^i| = c\sqrt{B} / \hat{n}_o$.
The analysis of expressions (133)--(135) shows that, when

$$\delta_{max}^2 = \hat{n}_o \zeta' / \hat{p}_e^0, \qquad \Delta a_e^{max} = -|\zeta''|^2 / \kappa_e, \tag{136}$$

a conversion occurs (r_{ee} = 0); i.e., the amplitude of the extraordinary reflected wave strictly vanishes. As a result, again a pumped polariton--plasmon arises in which the primary mode is the localized mode (an ordinary polariton in the crystal and a plasmon in the metal) whose intensity on the interface is much greater than the intensity of the incident pumping wave, which is clear from the expression for the absolute maximum of the excitation factor:

$$K_{oe}\left(\delta_{max}^2, \Delta a_e^{max}\right) \equiv \; K_{oe}^{max} = \hat{p}_e^0 \hat{n}_o / \varepsilon_e \zeta' \sqrt{B}. \tag{137}$$

Substituting here $\hat{p}_e^0 = |c_3|\sqrt{\gamma - 1}$, we can easily see that again the factor K_{oe}^{max} is optimized for c_1 = 0 when $c_3 \approx 1$. In this case,

$$K_{eo}^{max} = \frac{1}{\zeta'}\sqrt{\frac{\varepsilon_e - \varepsilon_o}{\varepsilon_o \varepsilon_e}}. \tag{138}$$

Formulas (138) and (126) turn into each other under the interchange $e \leftrightarrow o$.
The penetration depth of the polariton into the crystal in the pumped configuration is

$$d_o = \lambda_0 / 2\pi\varepsilon_o |\zeta''|. \tag{139}$$

In the neighborhood of coordinates (136) of the absolute maximum (137), a peak of the excitation factor $K_{oe}(\delta^2, \Delta a_e)$ is formed whose configuration is qualitatively correctly illustrated in Figs. 8 and 9. The half-widths of the curves that arise in two sections of this peak $\Delta a_e \equiv \Delta a_e^{max}$ and $\delta^2 \equiv \delta_{max}^2$ are, respectively, given by

$$(\Delta\delta^2)_{1/2} = 4\sqrt{2}\hat{n}_o \zeta' / \hat{p}_e^0, \quad (\Delta a_e)_{1/2} = 8\zeta' |\zeta''| / \kappa_e. \tag{140}$$

The excitation resonance of a bulk polariton in the crystal for $\Delta a_e \geq 0$ is also completely analogous to the resonance described above. Again the excitation factor is the larger, the smaller is the deviation angle Δa_e, and again a peak arises with respect to δ^2:

$$K_{oe}(\delta^2, 0) = \frac{4\delta^2 (\hat{p}_e^0)^2 / \varepsilon_e \sqrt{B}}{(\delta^2 \hat{p}_e^0 / \hat{n}_o + \zeta')^2 + \zeta''^2}, \tag{141}$$

the coordinate of whose maximum is given by

$$\bar{\delta}^2_{max} = \hat{n}_o \,|\, \zeta \,| \,/ \hat{p}^0_e \approx \hat{n}_o \,|\, \zeta'' \,| \,/ \hat{p}^0_e \,, \tag{142}$$

and the peak height (the absolute maximum) is given by an analog of (125):

$$\bar{K}^{max}_{oe} = K_{oe}(\bar{\delta}^2_{max}, 0) \approx 2\hat{n}_o \hat{p}^0_e \,/\, \varepsilon_e \sqrt{B}(|\, \zeta'' \,| + \zeta') \,. \tag{143}$$

As above, the choice of the geometry $c_1 = 0$ optimizes the factor $\bar{K}^{max}_{eo}$ and reduces (143) to the following analog of (126):

$$\bar{K}^{max}_{eo} = \frac{2}{|\, \zeta'' \,| + \zeta'} \sqrt{\frac{\varepsilon_e - \varepsilon_o}{\varepsilon_o \varepsilon_e}} \,. \tag{144}$$

The maximum intensity (143), (144) of the bulk wave attained for $\Delta a_e = 0$ is again accompanied by zero integral energy in this wave, because the main part of the incident extraordinary wave (except for the absorption in metal) is transferred to a reflected extraordinary wave. However, as is shown in Subsection 5.5, even a small increase in the angle of incidence from the value $\Delta a_e = 0$ substantially improves the energy distribution between reflected waves with a small loss in the amplitude of the excitation factor. This fact can easily be verified quantitatively by analyzing formulas (127) and (128) upon the interchange of the indices $o \leftrightarrow e$.

6. Recommendations for setting up an experiment

The resonance discussed is completely attributed to the anisotropy of the crystal and the shielding of the wave field in the crystal by metallization of the surface. Therefore, one should choose a crystal with large anisotropy factor $|\, \gamma \text{ -- } 1 \,|$ and a metal with low surface impedance ζ. This will guarantee the maximum intensity of the wave excited during reflection (see formulas (112), (140) and (128), (145)).

The orientation of the working surfaces of a sample is determined by the optical sign and the permittivities of the crystal and by the impedance of the metal coating at a given wavelength. As shown above, the optical axis should be chosen to be orthogonal to the propagation direction x: $c_1 = 0$ (Fig. 1). In optically positive and negative crystals, this axis should make angles of θ_{max} and 90° -- θ_{max}, respectively, with the metallized surface. When a *surface* polariton--plasmon is excited in an optically *positive* crystal, we have

$$\theta_{max} = \arctan\delta_{max} \,, \qquad \delta^2_{max} = \frac{\zeta' \varepsilon_o}{\sqrt{\varepsilon_e - \varepsilon_o}} \,. \tag{145}$$

If the goal of the experiment is to obtain an intense *bulk* reflected wave, then one should change δ^2_{max} to $\bar{\delta}^2_{max} = \delta^2_{max} \zeta'' \,| \,/ \zeta'$ (i.e., $\zeta' \to |\, \zeta'' \,|$) and $\theta_{\max}$ to $\bar{\theta}_{max}$ in (145). For optically *negative* crystals, appropriate angles $\theta_{\max}$ and $\bar{\theta}_{max}$ are defined by the same formulas (145) in which the indices o and e should be interchanged. For sodium nitrate crystals, the angles $\theta_{\max}$ and $\bar{\theta}_{max}$ are given in Table 2.

In an optically *positive* crystal in which a *surface* polariton--plasmon is excited, the input surface for a normally incident initial wave should be cut at the angle

$$a_e = \hat{a}_e + \Delta a_e^{max}, \qquad \hat{a}_e = \arctan\sqrt{\frac{(\gamma-1)(1+\delta_{max}^2)}{1+\gamma\delta_{max}^2}}, \qquad \Delta a_e^{max} = -\frac{|\zeta''|^2\,\varepsilon_o}{2\sqrt{\gamma-1}}. \tag{146}$$

In the case of excitation of a *bulk* polariton, one should make the following changes in (146): $\hat{a}_e \to \bar{\hat{a}}_e$ and $\delta_{max}^2 \to \bar{\delta}_{max}^2$. The expressions for $\hat{a}_e$ and $\bar{\hat{a}}_e$ following from (146) are exact. We did not decompose them with respect to the parameters δ_{max}^2 and $\bar{\delta}_{max}^2$, because they are not small enough at some wavelengths. To successfully observe a resonance, one should determine the angles of incidence as precisely as possible, especially when the angular width of the resonance is small.

In an optically *negative* crystal, instead of (146) we have

$$a_o = \hat{a}_o + \Delta a_o^{max}, \qquad \hat{a}_o = \arctan\sqrt{1/\gamma - 1}, \qquad \Delta a_o^{max} = -\frac{|\zeta''|^2\,\varepsilon_o}{2\sqrt{1/\gamma-1}}. \tag{147}$$

Here the limiting angle $\hat{a}_o$ is insensitive to the perturbation of c_3, being the same for the excitation of localized and bulk polaritons (see Table 2).

The output surface for the excited *bulk* wave should be orthogonal to its refraction vector, determined in an optically positive or negative crystal by the angle β_o or β_e (Figs. 2a and 7b):

$$\beta_o = \arctan\left(|\zeta''|\sqrt{\varepsilon_o}\right), \qquad \beta_e = \arctan\left(|\zeta''|\sqrt{\varepsilon_e}/\gamma\right). \tag{148}$$

For optically negative crystals, the angle β_e is naturally different from the slope angle ϕ_e of its ray velocity $\mathbf{u}_e$ in the reflected beam (see Figs. 7b and 11).

A correct choice of the polarization of the incident laser beam allows one to avoid the occurrence of a parasitic beam as a result of birefringence at the input of the crystal, i.e., additional loss of the energy of the incident beam. According to (45) and (50) for $c_1 = 0$, the polarization of the wave at the input should be of *TE* type in zero approximation ($\delta = 0$): the field $\mathbf{e}^i$ is parallel to the z axis for crystals of both optical signs. In a more precise analysis ($\delta = \delta_{max}$), the polarization vector $\mathbf{e}^i$ should be turned (about the vector $\mathbf{n}^i$) through an angle ψ. When exciting a *surface* polariton--plasmon, in the first approximation this angle is given by

$$\psi \approx \arctan(\delta_{max}/\sqrt{\gamma}); \tag{149}$$

in optically negative crystals, this rotation is clockwise, whereas, in optically positive crystals, counterclockwise. Table 2 shows that the angle ψ is small.

The situation is changed when one deals with the excitation of a *bulk* wave. Now the optimized polarization of the incident wave is defined by the same Eq. (149) in which δ_{max} is replaced by $\bar{\delta}_{max}$. In this case, the rotation angle ψ sharply increases, while the accuracy of approximation substantially degrades (at least for the visible range). It seems that in this case it is better to choose an optimal polarization of the initial wave experimentally.

As we have seen, the resonance width with respect to the angle of incidence sharply decreases when passing to the infrared region to values of $(\Delta a_{o,e})_{1/2} \approx 0.1$. This imposes a constraint on the divergence of the initial laser beam: the higher the divergence of a beam, the larger part of this beam goes out of resonance. One should also take into account that, by narrowing down the beam at the input, we increase its natural diffraction divergence.

7. Acknowledgements

This work was supported by the Polish Foundation MNiSW, project no. NN501252334. One of the authors (V.I.A.) acknowledges the support of the Polish--Japanese Institute of Information Technology, Warsaw, and the Kielce University of Technology, Poland.

8. References

Agranovich, V.M. (1975). Crystal optics of surface polaritons and the properties of surfaces. *Usp. Fiz. Nauk*, Vol. 115, No. 2 (Feb., 1975) 199-237, ISSN 0042-1294 [*Sov. Phys. Usp.*, Vol. 18, No. 2, (1975) 99-117, ISSN 1063-7859]

Agranovich, V.M. & Mills, D.L. (Eds.) (1982). *Surface Polaritons: Electromagnetic Waves at Surfaces and Interfaces*, North-Holland, ISBN 0444861653, Amsterdam

Alshits, V.I.; Gorkunova, A.S.; Lyubimov, V.N.; Gierulski, W.; Radowicz, A. & Kotowski, R.K. (1999). Methods of resonant excitation of surface waves in crystals, In: *Trends in Continuum Physics (TRECOP '88),* B.T. Maruszewski, W. Muschik & A. Radowicz, (Eds.), pp. 28-34, World Scientific, ISBN 981023760X, Singapore.

Alshits, V.I. & Lyubimov, V.N. (2002a). Dispersionless surface polaritons in the vicinity of different sections of optically uniaxial crystals. *Fiz. Tverd. Tela (St. Petersburg)*, Vol. 44, No. 2 (Feb., 2002) 371-374, ISSN 0367-3294 [*Phys. Solid State*, Vol. 44, No. 2 (2002) 386-390, ISSN 1063-7834]

Alshits, V.I. & Lyubimov, V.N. (2002b). Dispersionless polaritons on symmetrically oriented surfaces of biaxial crystals. *Fiz. Tverd. Tela (St. Petersburg)*, Vol. 44, No. 10 (Oct., 2002) 1895-1899, ISSN 0367-3294 [*Phys. Solid State*, Vol. 44, No. 10 (2002) 1988-1992, ISSN 1063-7834]

Alshits, V.I. & Lyubimov, V.N. (2005). Dispersion polaritons on metallized surfaces of optically uniaxial crystals. *Zh. Eksp. Teor. Fiz.*, Vol. 128, No. 5 (May, 2005) 904-912, ISSN 0044-4510 [*JETP*, Vol. 101, No. 5 (2005) 779-787, ISSN 1063-7761]

Alshits, V.I. & Lyubimov, V.N. (2009a). Generalization of the Leontovich approximation for electromagnetic fields on a dielectric – metal interface. *Usp. Fiz. Nauk*, Vol. 179, No. 8, (Aug., 2009) 865-871, ISSN 0042-1294 [Physics – Uspekhi, Vol. 52, No.8 (2009) 815-820, ISSN 1063-7859]

Alshits, V.I. & Lyubimov, V.N. (2009b). Bulk polaritons in a biaxial crystal at the interface with a perfect metal. *Kristallografiya*, Vol. 54, No. 6 (Nov., 2009) 989-993, ISSN 0023-4761 [*Crystallography Reports*, Vol. 54, No. 6 (2009) 941-945, ISSN 1063-7745]

Alshits, V.I.; Lyubimov, V.N. (2010). Resonance excitation of polaritons and plasmons at the interface between a uniaxial crystal and a metal. *Zh. Eksp. Teor. Fiz.*, Vol. 138, No. *4* (*Oct.,* 2010) 669-686, ISSN 0044-4510 [*JETP*, Vol. 111, No. *4* (2010) 590-606, ISSN 1063-7761]

Alshits, V.I.; Lyubimov, V.N. & Radowicz, A. (2007). Electromagnetic waves in uniaxial crystals with metallized boundaries: mode conversion, simple reflections, and bulk polaritons. *Zh. Eksp. Teor. Fiz.*, Vol. 131, No. 1 (Jan., 2007) 14-29, ISSN 0044-4510 [*JETP*, Vol. 104, No. 1 (2007) 9-23, ISSN 1063-7761]

Alshits, V.I. ; Lyubimov, V.N. & Shuvalov, L.A. (2001). Pseudosurface dispersion polaritons and their resonance excitation. *Fiz. Tverd. Tela (St. Petersburg)*, Vol. 43, No. 7 (Jul., 2001) 1322-1326, ISSN 0367-3294 [*Phys. Solid State*, Vol. 43, No. 7 (2001) 1377-1381, ISSN 1063-7834]

Born, M. & Wolf, E. (1986). *Principles of Optics*, Pergamon press, ISBN 0.08-026482.4, Oxford

Depine, R.A. & Gigli, M.L. (1995). Excitation of surface plasmons and total absorption of light at the flat boundary between a metal and a uniaxial crystal. *Optics Letters*, Vol. 20, No. 21 (Nov., 1995) 2243-2245, ISSN 0146-9592

D'yakonov, M.I. (1988). New type of electromagnetic wave propagating at the interface. *Zh. Eksp. Teor. Fiz.*, Vol. 94, No. 4 (Apr., 1988) 119-123, ISSN 0044-4510 [*Sov. Phys. JETP,* Vol. 67, No. 4 (1988) 714-716, ISSN 1063-7761]

Fedorov, F.I. (2004). *Optics of Anisotropic Media* (in Russian), Editorial URSS, ISBN 5-354-00432-2, Moscow

Fedorov, F.I. & Filippov, V.V. (1976). *Reflection and Refraction of Light by Transparent Crystals* (in Russian), Nauka I Tekhnika, Minsk

Furs, A.N. & Barkovsky, L.M. (1999). General existence conditions for polaritons in anisotropic, superconductive and isotropic systems *J. Opt. A: Pure Appl. Opt.,* Vol. 1 (Jan., 1999) 109-115, ISSN 1464-4258

Landau, L.D. & Lifshitz, E.M. (1993) *Electrodynamics of Continuous Media*, Butterworth-Heinemann, ISBN, Oxford

Lyubimov, V.N.; Alshits, V.I.; Golovina, T.G.; Konstantinova, A.F. & Evdischenko, E.A. (2010). Resonance and conversion reflections from the interface between a crystal and a metal. *Kristallografiya*, Vol. 55, No. 6 (Nov., 2010) 968-974, ISSN 0023-4761 [*Crystallography Reports*, Vol. 55, No. 6 (2010) 910-916 ISSN 1063-7745]

Marchevskii, F.N.; Strizhevskii, V.L. & Strizhevskii, S.V. (1984). Singular electromagnetic waves in bounded anisotropic media *Fiz. Tverd. Tela (St. Petersburg)*, Vol. 26, No. 5 (*May*, 1984) 1501-1503, ISSN 0367-3294 [*Sov. Phys. Solid State*, Vol. 26, No. 5 (1984) 911-913, ISSN 1063-7834]

Motulevich G.P. (1969). Optical properties of polyvalent non-transition metals. *Usp. Fiz. Nauk*, Vol. 97, No. 2 (Jan., 1969) 211-256, ISSN 0042-1294 [*Sov. Phys. Usp.,* Vol. 12, North-Holland, No. 1, 80-104, ISSN 1063-7859]

Sirotin, Yu.I. & Shaskol'skaya, M.P. (1979). *Fundamentals of Crystal Physics* (in Russian), Nauka, Moscow [(1982) translation into English, Mir, ISBN , Moscow]

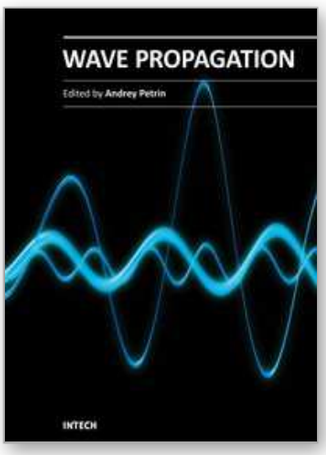

Wave Propagation
Edited by Dr. Andrey Petrin

ISBN 978-953-307-275-3
Hard cover, 570 pages
Publisher InTech
Published online 16, March, 2011
Published in print edition March, 2011

The book collects original and innovative research studies of the experienced and actively working scientists in the field of wave propagation which produced new methods in this area of research and obtained new and important results. Every chapter of this book is the result of the authors achieved in the particular field of research. The themes of the studies vary from investigation on modern applications such as metamaterials, photonic crystals and nanofocusing of light to the traditional engineering applications of electrodynamics such as antennas, waveguides and radar investigations.

How to reference
In order to correctly reference this scholarly work, feel free to copy and paste the following:

V.I. Alshits, V.N. Lyubimov, and A. Radowicz (2011). Electromagnetic Waves in Crystals with Metallized Boundaries, Wave Propagation, Dr. Andrey Petrin (Ed.), ISBN: 978-953-307-275-3, InTech, Available from: http://www.intechopen.com/books/wave-propagation/electromagnetic-waves-in-crystals-with-metallized-boundaries

INTECH
open science | open minds

InTech Europe
University Campus STeP Ri
Slavka Krautzeka 83/A
51000 Rijeka, Croatia
Phone: +385 (51) 770 447
Fax: +385 (51) 686 166
www.intechopen.com

InTech China
Unit 405, Office Block, Hotel Equatorial Shanghai
No.65, Yan An Road (West), Shanghai, 200040, China
中国上海市延安西路65号上海国际贵都大饭店办公楼405单元
Phone: +86-21-62489820
Fax: +86-21-62489821

IntechOpen